ADVANCES IN INORGANIC CHEMISTRY, VOL. 32

THE REDOX CHEMISTRY OF NICKEL

A. GRAHAM LAPPIN* and ALEXANDER McAULEY**

* Department of Chemistry, University of Notre Dame, Notre Dame, Indiana 46556, and
** Department of Chemistry, University of Victoria, Victoria, British Columbia, Canada V8W 2Y2

I. Introduction

The discovery of nickel(III) (*1–7*) and nickel(I) (*8*) in methanogenic bacteria and in other biological systems has focused attention on the redox chemistry of nickel. For many years, this aspect of the coordination chemistry of nickel was largely overlooked but facile oxidation and reduction extends from formal nickel(IV) species to formal nickel(I) species, encompassing structural requirements of the electronic configurations d^6–d^9. There exists a wealth of information on the requirements for stabilization of these electronic configurations for nickel and the area has been reviewed relatively recently (*9, 10*). In this article, the most recent advances are emphasized, particularly those where structural characterization is relatively unambiguous and where the work has been pursued to some conclusion. The area covered is fairly selective, thus ligands with phosphorus, arsenic, and dithiolate coordination have been excluded, as they are reviewed in detail elsewhere (*9*).

The article is organized around a discussion of the structural and electronic requirements of the four oxidation states, I, II, III, and IV,

and of the primary physical techniques and probes used. A description of the most commonly used ligand types follows, together with an indication of recent trends in the area. Each section concludes with a review of the recent mechanistic chemistry of the oxidation states in turn. A glossary of ligand abbreviations is included at the end of the review.

II. Steric and Electronic Requirements

The starting point for most of the redox chemistry considered in this review is the nickel(II) ion. The nickel(II) ion has a d^8 electronic configuration and, with weak-field ligands such as H_2O, it forms a six-coordinate ion with approximately octahedral symmetry and a paramagnetic (two unpaired electrons) $^3A_2$ ground state. The characteristic solution chemistry of six-coordinate nickel(II) is well documented and, in particular, the substitution behavior has been extensively studied and is the subject of recent reviews (*11, 12*). It is a labile ion with solvent exchange rates around 10^4 sec^{-1} at 25°C and activation parameters are consistent with dissociatively activated interchange behavior (*13*).

Thermodynamic stability of the six-coordinate complexes generally increases as the ligand-field strength increases. For stronger field chelating ligands such as phen or bpy, the tris complexes can be resolved into optical isomers (*14*). Rates of racemization correspond to rates of ligand exchange, 1.6×10^{-4} sec^{-1} for $[Ni(phen)_3]^{2+}$ at 45°C, indicating that complete dissociation of a ligand is required before rearrangement can occur (*15*).

Addition of ligand systems capable of producing a strong square–planar ligand field results in formation of the diamagnetic $^1A_{1g}$ ground state which shows extensive ligand-field stabilization and consequent sluggish substitution behavior by mechanisms which tend to be associative in nature (*11*).

The importance of these two dominant complex geometries for nickel(II) becomes apparent on examination of the stereoelectronic requirements for the oxidized and reduced metal species. Both nickel(I), d^9, and nickel(III), d^7, which is generally found as a low-spin species because of the increased charge on the metal ion, are subject to Jahn–Teller distortion and hence have a strong preference for tetragonal geometry, intermediate between octahedral and square–planar geometry and readily accessible from both. In contrast, nickel(IV), d^6, again generally low spin, has a strong preference for octahedral

geometry, analogous to cobalt(III), and is difficult to form from a square–planar nickel(II) complex. Thus consideration of the geometry of the nickel(II) complex can lead to control of the ultimate oxidation state of the species on oxidation or reduction.

Clearly different ligand types will favor different oxidation states. Higher oxidation states prefer hard acid donor atoms, generally first-row *p*-block elements, rich in electron density and capable of strong σ donation. A further provision is that they should resist oxidation. Common donor chromophores which have been used are amines $\geqslant$N, imides (including oximes and imines)$>N^-$, oxides $—O^-$ and fluorides F^-. Second- and third-row *p*-block donors have also been used, forming bonds which are more covalent in character and creating special problems, as discussed below.

The nickel(I) state is favored by soft donors capable of π back bonding. Although there is a rich chemistry associated with second- and third-row *p*-block donors to nickel(I), examples in this review will be restricted again to, primarily, nitrogen and oxygen as donor atoms.

On addition or removal of an electron from a nickel(II) complex, there is frequently a problem in deciding whether redox has occurred at the metal center in which case the ligand is an "innocent" bystander to the process or whether ligand centered redox has occurred, so-called "noninnocent" behavior. This problem has plagued the literature, particularly dealing with the higher oxidation states of nickel and there are proposals for deciding between the two possibilities, some of which are outlined in the next section. Clearly, however, this is a question of semantics. Every "metal-centered" oxidation or reduction involves accommodation on the part of the ligand. Some charge redistribution undoubtedly occurs. A good rule of thumb is that the products of ligand-centered oxidation or reduction will show characteristics of radicals while the products of metal-centered oxidation will show characteristics expected of isoelectronic metal ion complexes. Thus nickel(IV) chemistry should be similar to the chemistry of cobalt(III), nickel(III) chemistry should resemble that of low-spin cobalt(II), and nickel(I) that of copper(II). For the types of donors considered in this review, these similarities are indeed borne out.

III. Probes of Structure

The X-ray crystal structures of a variety of high- and low-oxidation-state nickel complexes are now known. These are introduced throughout the text in Section IV,A and the important points are summarized in

Section IV,A,5. In a number of instances, structures of the corresponding nickel(II) complexes are also known, allowing direct comparisons of metal–ligand bond lengths, and bond lengths and angles within the ligand, important in deciding whether redox is metal centered or ligand centered. If, on oxidation, metal–ligand bond lengths contract but those within the ligand are largely unaffected, then oxidation is thought to be primarily metal centered.

The technique most widely applied as a structural probe in the chemistry of both nickel(III) and nickel(I) is electron paramagnetic resonance. The g value is a function of the spin-orbit coupling constant and the ligand-field splitting, and is anisotropic. From frozen glasses of the complexes, the order of the g values gives detailed structural information (see Fig. 1), allowing distinction between tetragonal and square–planar geometry (*16*). In a square–planar geometry $g_{zz} > g_{xx}, g_{yy}$, similar to that found in a tetragonally compressed geometry but quite different from the situation for a tetragonally elongated geometry where $g_{xx}, g_{yy} > g_{zz} \approx 2$. For nickel(I) the situation is effectively reversed (*17*) since the unpaired electron is in a $d_{x^2-y^2}$ orbital in both tetragonally elongated and square–planar geometries, and in a d_{z^2} orbital for the tetragonally compressed case. Hyperfine interactions can also be used in assigning ligand donor atoms.

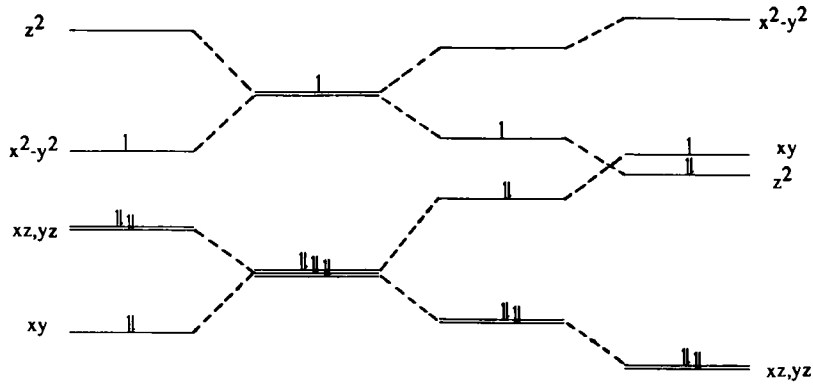

FIG. 1. The splitting of the d orbitals in tetragonally compressed, tetragonally elongated, and square–planar geometric for a d^7 ion and the resulting relative g values for d^7 and d^9 configurations.

With first-row *p*-block donor atoms, ligand radical species produced by ligand-centered redox processes tend to have isotropic *g* values close to the *g* value for a free electron, 2.0023, because the atoms in which the electron resides have no orbital contribution to paramagnetism (spin-orbit coupling is small compared with differences in the electronic energy levels). Thus, both the anisotropy and the magnitude of the *g* values of nickel(III) and nickel(I) complexes can be taken to indicate the degree of metal-centered oxidation or reduction. For nickel(III) complexes, Drago (*18*) has suggested (somewhat arbitrarily) a cutoff of 2.06 for the average *g* values, $\langle g \rangle$, to distinguish between metal-centered and ligand-centered oxidation. Nickel(IV) complexes are not amenable to study by EPR methods since, in general, they are diamagnetic. Nuclear magnetic resonance studies are possible, but thus far, results are few.

There is no generalized treatment of the UV/visible spectra of these complexes since they tend to be dominated by low-energy charge transfer bands which obscure details of the d–d structure. In a few instances, circular dichroism data have been reported, but detailed interpretation has not been attempted (*19*).

IV. Oxidation of Nickel(II)

A. Coordination Environments and Structural Chemistry

1. Amines, Imines, and Oximes

Saturated amines provide a ligand field significantly greater than that of water and allow oxidation of nickel(II) under a variety of conditions. Early studies in this area involved pulse radiolysis (*20, 21*) and electrochemical (*22*) oxidation of nickel(II) in solutions of ammonia and 1,2-diaminoethane (en). The bis complex $[Ni^{II}(en)_2Cl_2]$ can be oxidized by chlorine in methanolic solution to give [*trans*-$Ni^{III}(en)_2Cl_2]Cl$, which has a magnetic moment of 1.90 BM and shows (*23*) an axial EPR Spectrum (Table I), consistent with tetragonally elongated nickel(III). Hyperfine coupling from two axially bound chlorine nuclei is resolved in HCl solutions (*24*) and, interestingly, sulfate ion has a marked stabilizing effect on the complex. The chemistry of $[Ni^{III}(en)_2Cl_2]Cl$ resembles the chemistry of the nickel(III) complexes of tetraazamacrocycles discussed in Section IV,A,2.

Under milder oxidation conditions a different product is formed (*25, 26*), best formulated as $[Ni^{II}(en)_2Ni^{IV}(en)_2Cl_2]Cl_4$. The magnetic moment is reduced to 0.76 BM and there is an intense intervalence band

TABLE I

SELECTED EPR DATA FOR NICKEL(III) COMPLEXES

Complex	Medium	g_{xx}	g_{yy}	g_{zz}	A_{xx} (G)	A_{yy} (G)	A_{zz} (G)	Reference
$[Ni^{III}(en)_2Cl_2]^+$	Aq. HCl, 77 K	2.165	2.165	2.017	—	—	30	*24*
$[Ni^{III}(bpy)_3]^{3+}$	CH_2CN, 77 K	2.137	2.137	2.027	15	15	22.2	*31*
$[Ni^{III}(phen)_3]^{3+}$	CH_3CN, 77 K	2.136	2.137	2.027	16	16	23.2	*31*
$[Ni^{III}(bpo)_3]$	Solid	2.14	2.10	2.08	—	—	—	*18*
$[Ni^{III}(dmg)_3]^{3-}$	Base, 77 K	2.17	2.17	2.03	—	—	23.6	*36*
$[Ni^{III}Me_2L]^+$	Aq., 77 K	2.155	2.155	2.033	—	—	—	*56*
$[Ni^{III}Me_2LH]^{2+}$	Single crystal	2.1521	2.1289	2.0464	—	—	—	*59*
$[Ni^{III}Me_2L']$	Aq., 77 K	2.134	2.134	2.030	—	—	—	*60*
$[Ni^{III}DOHDOpnCl_2]$	Doped solid	2.155	2.143	2.026	11	11	65	*61*
$[Ni^{III}[12]aneN_4]^{3+}$	CH_3CN, 77 K	2.06	2.06	2.17	—	—	—	*73*
$[Ni^{III}[14]aneN_4]^{3+}$ [a]	CH_3CN, 77 K	2.20	2.20	2.03	—	—	41	*73*
$[Ni^{III}[14]aneN_4]^{3+}$ [a]	CH_3CN, 77 K	2.2148	2.2148	2.0250	—	—	—	*75*
$[Ni^{III}[14]aneN_4]^{3+}$ [a]	H_2O, 77 K	2.2193	2.2193	2.0332	—	—	—	*75*
$[Ni^{III}[14]aneN_4]^{3+}$ [a]	DMSO, 77 K	2.242	2.242	2.026	—	—	—	*74*
$[Ni^{III}[14]aneN_4(Cl)_2]^+$	DMSO, 77 K	2.180	2.180	2.022	<5	<5	28	*74*
$[Ni^{III}[15]aneN_5]^{3+}$ [b]	CH_3CN, 77 K	2.17	2.17	2.03	—	—	34	*73*
$[Ni^{III}[18]aneN_6]^{3+}$	CH_3CN, 77 K	2.16	2.16	2.06	—	—	—	*73*
$[Ni^{III}([9]aneN_3)_2]^{3+}$	Single crystal	2.12	2.12	2.03	—	—	—	*33*
$[Ni^{III}H_{-2}[14]dioxoaneN_4]^+$	H_2O, 77 K	2.23	2.23	2.02	—	—	—	*95*
$[Ni^{III}H_{-2}[16]dioxoaneN_5]^+$	H_2O, 77 K	2.154	2.154	2.016	—	—	21.7	*102*
$[Ni^{III}H_{-2}G_3]$	H_2O, 100 K	2.242	2.295	2.015	—	—	—	*118*
$[Ni^{III}H_{-3}G_4]^-$	H_2O, 100 K	2.297	2.278	2.010	—	—	—	*118*
$[Ni^{III}H_{-3}G_3a]$	H_2O, 100 K	2.310	2.281	2.006	—	—	—	*118*
$[Ni^{III}H_{-3}G_3a(NH_3)]$	H_2O, 100 K	2.217	2.217	2.011	—	—	23.4	*118*
$[Ni^{III}H_{-3}G_3a(NH_3)_2]$	H_2O, 100 K	2.178	2.178	2.019	—	—	19	*118*
$[Ni^{III}(H_{-1}G_2)_2]^-$	H_2O, 100 K	2.07	2.07	2.22	—	—	—	*124*
$[Ni^{III}(H_{-2}G_3)_2]^{3-}$	Base, 100 K	2.151	2.151	2.021	—	—	19.5	*125*
$[Ni^{III}(edta)]^-$	H_2O, 77 K	2.14	2.14	2.34	—	—	—	*129*
$[Ni^{III}(bpyO_2)_3]^{3+}$	CH_3CN, 77 K	2.220	2.155	2.060	—	—	—	*135*

[a] Other N_4 macrocycles are similar. [b] Other N_5 macrocycles are similar.

around 15,000 cm^{-1}. Resonance Raman studies (*27*) support a structure with an alternating Ni–Cl chain, consistent with the high electrical conductivity of the material. Interconversion of $[Ni^{III}(en)_2Cl_2]Cl$ and the mixed-valence form takes place in the presence of moisture (*28*).

The higher valent nickel complexes with saturated amine donors have little more than a transient existence as independent species in solution and consequently have a limited chemistry. Complexes with stronger donor ligands have a more extensive chemistry.

Oxidation of $[Ni^{II}(bpy)_3]^{2+}$ and other tris(polypyridyl) complexes is readily achieved electrolytically in 2 *M* $HClO_4$ (*29*) or in anhydrous acetonitrile (*30, 31*). The product, $[Ni^{III}(bpy)_3]^{3+}$, has a reduction potential of 1.72 V (versus normal hydrogen electrode, nhe) (Table II) showing an increasing trend with increasingly electronegative substituents on the polypyridine ligands. A weak absorption at 620 nm ($\varepsilon = 275\ M^{-1}\ cm^{-1}$) and a more intense shoulder at 400 nm ($\varepsilon_{350} = 5300\ M^{-1}\ cm^{-1}$) give the complex a lime-green color. The EPR data (*31*) with $g_{xx} = g_{yy} > g_{zz}$ (Table I) are interpreted in terms of a tetragonal elongation from octahedral symmetry with the unpaired electron in a d_{z^2} orbital and it is a little disconcerting that the X-ray structure of the complex (*32*) has two axial bonds 0.09 Å shorter than the average of the other four. Wieghardt and co-workers (*33*) have commented on this result, ruling out a dynamic in-plane distortion in favor of crystal packing forces. Whatever the explanation, it would appear that the energy barrier between elongated and compressed tetragonal distortion is not large. There is a significant (0.09–0.17 Å) shortening (*32, 34*) in the Ni–N bond lengths on going from $[Ni^{II}(bpy)_3]^{2+}$ to $[Ni^{III}(byp)_3]^{3+}$, while the ligand bond lengths and angles are little changed, indicating that oxidation is predominantly metal centered. These changes in Ni–N bond lengths contribute to the barrier to electron transfer between nickel(II) and nickel(III).

There is no evidence that oxidation of $[Ni^{III}(bpy)_3]^{3+}$ to give a nickel(IV) species can be effected. Likewise, when one of the pyridine rings is replaced by a benzoyl oxime as in *syn*-2-benzoylpyridine oxime (bpoH), oxidation, using persulfate in basic solution, is limited to

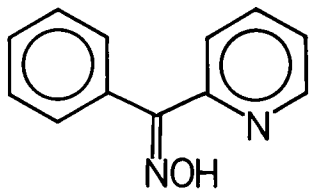

bpoH

1

TABLE II

REDUCTION POTENTIALS OF SELECTED NICKEL(III) COMPLEXES

Complex	$E^{0\,a}$			Reference
	CH_3CN^b	H_2O^c	0.5 M Na_2SO_4	
$[Ni^{III}(bpy)_3]^{3+}$	1.71	—	—	*31*
$[Ni^{III}(phen)_3]^{3+}$	1.73	—	—	*31*
$[Ni^{III}Me_2L']^{2+}$	—	0.65	—	*45, 56*
$[Ni^{III}Me_2L]^{+}$	—	0.42	—	*45, 56*
$[Ni^{III}Me_2LH]^{2+}$	—	0.64	—	*56*
$[Ni^{III}[12]aneN_4]^{3+}$	1.66	—	—	*73*
$[Ni^{III}[13]aneN_4]^{3+}$	1.28–1.48	—	—	*64, 73*
$[Ni^{III}[14]aneN_4]^{3+}$	1.28, 1.25	1.05, 0.99, 0.74[d]	0.744	*64, 73, 96, 146*
$[Ni^{III}iso[14]aneN_4]^{3+}$	1.42	—	—	*73*
$[Ni^{III}[15]aneN_4]^{3+}$	1.59, 1.48	—	1.014	*64, 73, 96*
$[Ni^{III}[16]aneN_4]^{3+}$	1.69	—	0.904	*73, 102*
$[Ni^{III}[15]aneN_5]^{3+}$	1.315	—	—	*73*
$[Ni^{III}[16]aneN_5]^{3+}$	1.35	—	—	*73*
$[Ni^{III}[17]aneN_5]^{3+}$	1.395	1.039	—	*73, 108*
$[Ni^{III}[18]aneN_6]^{3+}$	1.483	—	—	*73*
$[Ni^{III}([9]aneN_3)_2]^{3+}$	1.23	0.947, 1.015	—	*108, 146*
$[Ni^{III}([10]aneN_3)_2]^{3+}$	1.33	0.997, 1.014	—	*108, 146*

$[Ni^{III}([11]aneN_3)_2]^{3+}$	1.54	—	—	*108*
$[Ni^{III}H_{-2}[12]dioxoaneN_4]^{+}$	—	0.87	0.86	*96*
$[Ni^{III}H_{-2}[13]dioxoaneN_4]^{+}$	—	—	1.14	*96*
$[Ni^{III}H_{-2}[14]dioxoaneN_4]^{+}$	—	1.09, 0.89	1.05	*96*
$[Ni^{III}H_{-2}[15]dioxoaneN_4]^{+}$	—	1.16	0.86	*96*
$[Ni^{III}H_{-1}[16]oxoaneN_5]^{2+}$	—	—	0.70	*102*
$[Ni^{III}H_{-2}[16]dioxoaneN_5]^{+}$	—	—	0.48	*102*
$[Ni^{III}[14]aneN_4CH_2CH_2py]^{3+}$	—	—	0.74	*96*
$[Ni^{III}H_{-2}[13]dioxoaneN_4CH_2CH_2py]^{+}$	—	—	1.14	*96*
$[Ni^{III}H_{-2}[13]dioxoaneN_4CH_2CH_2pyO]^{+}$	—	—	0.87	*96*
$[Ni^{III}H_{-2}[14]dioxoaneN_4CH_2CH_2py]^{+}$	—	—	1.10	*96*
$[Ni^{III}[16]dioxoaneN_5CH_2CH_2py]^{3+}$	—	—	0.48	*102*
$[Ni^{III}H_{-2}G_3]$	—	0.85	—	*113*
$[Ni^{III}H_{-3}G_4]^{-}$	—	0.79	—	*113*
$[Ni^{III}H_{-3}G_3a]$	—	0.83	—	*113*
$[Ni^{III}(H_{-2}G_3)_2]^{3-}$	—	<0.24	—	*123*
$[Ni^{III}(bpyO_2)_3]^{3+}$	1.81	—	—	*135*

[a] Versus a normal hydrogen electrode. Various ionic media are used; see references for details.

[b] Corrected for normal hydrogen electrode from Ag/Ag^{+} by the addition of 0.578 V (Mann, C., and Barnes, K., "Electrochemical Reactions in Nonaqueous Systems." Dekker, New York, 1970.

[c] Generally with weakly coordinating media.

[d] $[Ni^{III}[14]aneN_4(Cl)_2]^{+}$.

formation of a neutral nickel(III) complex $[Ni^{III}(bpo)_3]$ in which all three oxime protons are dissociated (*18*). In this case, a well-defined rhombic EPR signal is recorded with $g_{zz} > g_{xx} \approx g_{yy}$ consistent with tetragonally compressed geometry. When the second pyridine is replaced by an oxime group, as in dimethylglyoxime ($dmgH_2$) or diphenylglyoxime ($dpgH_2$), the situation changes and both nickel(III) and nickel(IV) complexes are readily accessible, depending on the mode of preparation.

The reasons for this change in behavior on going from bpy to bpo^- and dmg^{2-} are not readily apparent since reduction potential data which would allow comparisons of the complexes are not available for all members of the series. The most obvious change is that the ligands differ in charge and that deprotonation parallels the ability of the complex to accept a loss of electrons.

The best characterized (*35–38*) of the oxidized nickel dimethylglyoximate species is $[Ni^{IV}(dmg)_3]^{2-}$, which can be obtained as the diamagnetic potassium, sodium, or barium salt. Preparation of

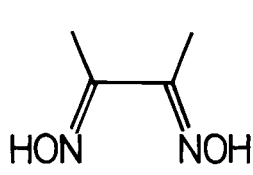

$dmgH_2$

2

$[Ni^{IV}(dmg)_3]^{2-}$ is best carried out by addition of dmg^{2-} to a basic suspension of the higher valent oxides or hydroxides in the presence of an oxidant, thereby avoiding formation of the insoluble, square-planar $[Ni(dmgH)_2]$. With weaker oxidants, varying amounts of less well-characterized nickel(III) species are produced (*39*).

Alkaline solutions of $[Ni(dmg)_3]^{2-}$ are relatively long lived and exhibit absorption maxima at 460, 365, and 285 nm (ε = 9600, 7200, and 4.8×10^4 M^{-1} cm^{-1}, respectively) (*33, 34*). The complex is inert to substitution as expected for a low-spin d^6 ion with a decomposition rate of 2.6×10^{-7} sec^{-1} at 35°C, but is sensitive to acid and protonates with a pK_a of 10.8 (*37*). A two-electron potential of 0.54 V (versus nhe) is reported (*38*) in 1.5 *M* NaOH but the data are questionable. One-electron reduction at pH 12.4 gives a paramagnetic intermediate (*36, 40*), presumably $[Ni^{III}(dmg)_3]^{3-}$, with absorption maxima (*41*) at 520 and 280 nm (ε = 3700 and 2.95×10^4 M^{-1} cm^{-1}), a different species from that formed (*42*) in the one-electron oxidation of $[Ni^{II}(dmgH)_2]$, which is likely to

have a lower coordination number. The EPR spectrum of the proposed $[Ni^{III}(dmg)_3]^{3-}$ is axial (*36*) with $g_{xx} = g_{yy} > g_{zz}$, consistent with an elongated tetragonal distortion. A similar signal has been identified in the iodine oxidation of the nickel(II) complex in pyridine solution (*39*). However, in such oxidation experiments, a large number of different EPR spectra are claimed, depending on experimental conditions, and details of the structures have not been elucidated. It is of interest to note that for the series $[Ni^{III}(bpy)_3]^{3+}$, $[Ni^{III}(bpo)_3]$, and $[Ni(dmg)_3]^{3-}$, the $\langle g \rangle$ value shows a modest increase from 2.10 to 2.12, perhaps signifying a slight increase in the degree of metal-centered oxidation. However, it is unlikely that this is important in increasing the accessibility of nickel(IV).

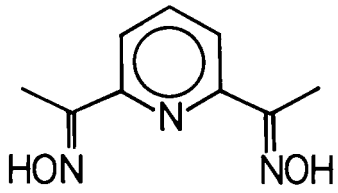

$dapdH_2$

3

In combination with other nitrogenous donor atoms, oximes have provided a particularly fruitful area for higher oxidation-state nickel chemistry. Tridentate coordination (*43*) in 2,6-diacetylpyridine dioxime ($dapdH_2$), which in its deprotonated form, $dapd^{2-}$, is a very strong field ligand, is used to suppress the formation of square–planar nickel(II). Persulfate oxidation of $[Ni^{II}(dapd)_2]^{2-}$ in basic media yields violet needles of the diamagnetic $[Ni^{IV}(dapd)_2]$. There is no evidence for the corresponding nickel(III) complex. The absorption spectrum of $[Ni^{IV}(dapd)_2]$ shows peaks at 630 and 450 nm. The complex is inert to substitution as evidenced by the observation that it can be dissolved in concentrated HNO_3. In the X-ray structure (*44*), the ligand distorts to accommodate the small nickel(IV) ion and the Ni–N bond distances are significantly shorter than in comparable complexes of nickel(II). A simple molecular orbital treatment (*43*) suggests that the concentration of negative charge in the donor nitrogen and oxime oxygens of $dapd^{2-}$ contributes to its ability to stabilize the higher oxidation states.

The most widely studied of the higher oxidation-state complexes incorporating oxime groups are those involving derivatives of the sexidentate ligand (*45, 46*) 3,14-dimethyl-4,7,10,13-tetraazahexadeca-

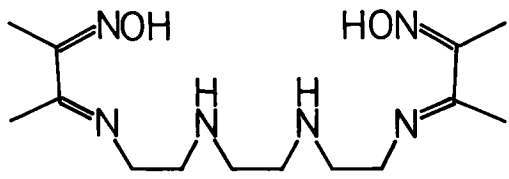

Me_2LH_2

4

3,13-diene-2,15-dione dioxime, Me_2LH_2. A variety of structural variations have been prepared (*47–50*), but they share the donor system comprising two oximes, two imines, and two amine nitrogen donors, and only the parent complex will be considered.

The nickel(II) complex $[Ni^{II}Me_2LH_2]^{2+}$ is a typical six-coordinate, high-spin species with a magnetic moment of 3.12 BM and undergoes successive deprotonation of the oxime oxygens with pK_a values of 5.90 and 7.80 (*45, 46*). Chemical or electrochemical oxidation results in the highly colored diamagnetic nickel(IV) species $[Ni^{IV}Me_2L]^{2+}$ in which both oxime groups are deprotonated. The X-ray structures of both $[Ni^{IV}Me_2L](ClO_4)_2$ and $[Ni^{II}Me_2LH_2](ClO_4)_2$ have been determined (*51–53*) and show significant changes in the Ni–N bond lengths. For the former complex, average Ni–N bond lengths are 1.955 (amine), 1.871 (imine), and 1.953 (oxime) Å, while for the latter they are longer, 2.098, 2.055, and 2.119 Å, respectively. Small changes in the ligand bond lengths and angles are also noted.

Wrapping the sexidentate ligand around the metal (Fig. 2) creates a pair of optical isomers and the nickel(IV) complexes are sufficiently inert to allow optical resolution (*54, 55*). UVvisible and circular dichroism spectra are shown in Fig. 3. Further evidence of the inert-

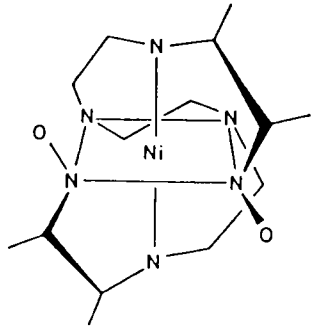

FIG. 2. $[Ni^{IV}Me_2L]^{2+}$

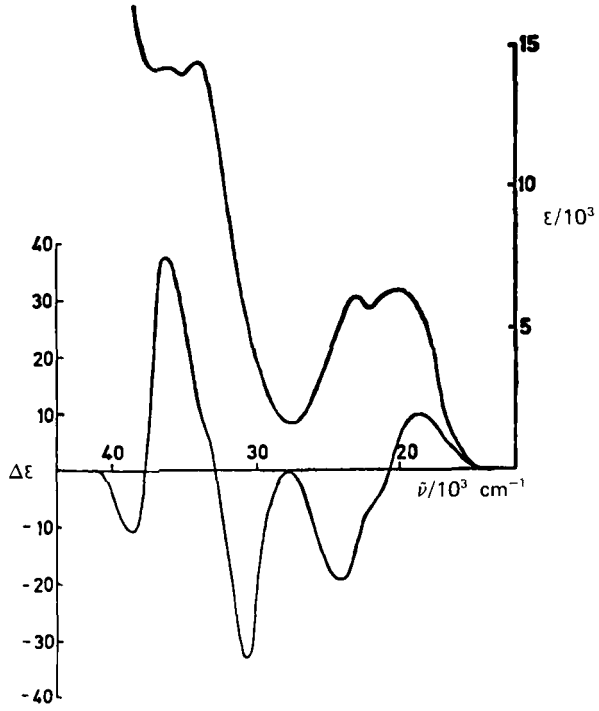

FIG. 3. Absorption and circular dichroism spectra of an aqueous solution of $[Ni^{IV}Me_2L]^{2+}$; from Ref. *54* by permission of the authors and the Royal Society of Chemistry.

ness to substitution of the nickel(IV) complex is provided by the fact that the ligand will not unwrap in concentrated HNO_3.

Above pH 5, the corresponding nickel(III) complex, $[Ni^{III}Me_2L]^+$, is thermodynamically stable (*56, 58*). It has an absorption spectrum similar to but less intense than that of $[Ni^{IV}Me_2L]^{2+}$, with maxima at 505 and 398 nm (ε = 2890 and 3000 M^{-1} cm^{-1}) (*56*). The EPR spectrum is typical of a tetragonally elongated complex with $g_{xx} = g_{yy} = 2.16$ and $g_{zz} = 2.04$. At lower pH a protonated form ($pK_a = 4.05$) $[Ni^{III}Me_2LH]^{2+}$ has been detected as a thermodynamically unstable kinetic transient with a broad absorption maximum at 490 nm (ε = 2980 M^{-1} cm^{-1}). Single-crystal EPR data (*59*) for this species are available and again a tetragonally elongated geometry is consistent with the data. The g values show a slight rhombic distortion with $g_{xx} = 2.1521$, $g_{yy} = 2.1289$, and $g_{zz} = 2.0464$, in good agreement with other determinations for this complex.

When one of the oxime–imime groups is replaced by two amine donors in the ligand $Me_2L'H$, oxidation is restricted to the trivalent

state (*60*), leading to the conjecture that a minimum of two oxime–imine chromophores are required to stabilize nickel(IV). The complex $[Ni^{III}Me_2L']^+$ is paramagnetic, showing an axial EPR spectrum with $g_{xx} = g_{yy} = 2.134$ and $g_{zz} = 2.030$. The reduction potential is slightly higher than that of the bis(oxime–imine) system. Incorporation of the bis(oxime–imine) chromophore in a ligand $(DOH)_2pn$, where the

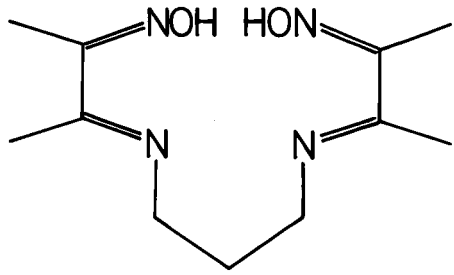

$(DOH)_2pn$

5

strong donors are restricted to a planar geometry, is also insufficient to stabilize nickel(IV) (*61*). The resulting nickel(III) complexes, $[Ni^{III}(DOH)(DO)pnCl_2]$ and $[Ni^{III}(DOH)(DO)pnBr_2]$, are tetragonally elongated and show axial hyperfine coupling from the halide ions.

2. *Macrocycles*

Complexes with macrocyclic ligands have a rich chemistry for both higher and lower oxidation states of nickel (*62–66*). The smallest members of the series, the triaza macrocycles, show no redox chemistry for 1:1 complexes with nickel(II), but there are recent reports of stable bis complexes which will be discussed later in this section.

The restricted geometry of the tetraaza macrocyclic ligands favors the formation of low-spin, square–planar nickel(II). An equilibrium exists between the blue, high-spin, six-coordinate form and the yellow, substitution-inert, square–planar form [Eq. (1)]. Intercoversion

$$\underset{\substack{\text{blue,}\\\text{high spin}}}{[Ni^{II}[14]aneN_4(H_2O)_2]^{2+}} \rightleftharpoons \underset{\substack{\text{yellow,}\\\text{low spin}}}{[Ni^{II}[14]aneN_4]^{2+}} + 2H_2O \qquad (1)$$

between the forms is dependent on structure (*67–70*), as shown in Table III, and appears to reflect a balance between exothermic solvent release and endothermic Ni–N bond shortening. Typical Ni–N

TABLE III

EQUILIBRIUM CONSTANTS AND THERMODYNAMIC PARAMETERS FOR THE BLUE-YELLOW INTERCONVERSION OF NICKEL(II) COMPLEXES

Ligand	K_{eq}	ΔG^0 (kcal mol^{-1})	ΔH^0 (kcal mol^{-1})	ΔS^0 (cal K^{-1} mol^{-1})	Reference
2,3,2-tet	0.3	0.7	3.4	9	*68*
2,2,2-tet	0.01	2.6	3.4	3	*67*
[14]aneN$_4$	1.6	−0.26	5.3	18.7	*68*
iso[14]aneN$_4$	2.3	−0.5	5.4	20	*70*
[13]aneN$_4$	68	−1.14	7.5	30	*69*
[12]aneN$_4$	0.8	0.1	1.7	5.5	*69*
Me$_2$[14]aneN$_4$	0.4	0.5	—	—	*140*
[12]dioxoaneN$_4$ [a]	6.7	−1.13	8.7	33	*94*
[13]dioxoaneN$_4$	0.5	0.4	4.2	12.8	*94*

[a] 1,2-Dioxo derivative.

bond lengths for high-spin nickel(II) are 2.1–2.2 Å and for low-spin nickel(II) are 1.9–2.0 Å. Rates of interconversion between the two forms, estimated from studies with linear tetraamines, are rapid (*71*), $>10^5$ sec^{-1} at 5°C.

Early studies of the oxidation of nickel(II) in saturated tetraaza macrocycles were carried out using electrochemical methods in acetonitrile solutions (*62, 64*). The nickel(III) state is readily accessible but removal of a second electron is not possible except in a few instances where ligand oxidation is involved. The reduction potentials of a variety of nickel(III) macrocyclic complexes are shown in Table II. One important feature in stabilizing nickel(III) is the hole size supported by the macrocycle (*64, 72, 73*). The complex with the symmetric 14-membered ring ligand, [14]aneN$_4$, is most thermodynamically stable, with an ideal Ni–N bond length of 2.07 Å. However, the asymmetric isomer, iso[14]aneN$_4$, is significantly less stable (*70*), illustrating the importance of ring configuration. It is noteworthy that the square-planar component of the ligand-field splitting parameter is smaller for [Ni^{II}iso[14]aneN$_4$]$^{2+}$ than for [Ni[14]aneN$_4$]$^{2+}$.

Most structural characterization of these complexes has been carried out by EPR methods (*64, 73–76*) and, with a few notable exceptions, the nickel(III) species show the expected elongated tetragonal geometry with axial coordination of solvent or counterions confirmed by hyperfine interactions (Table I). The smallest member of the tetraaza macrocycle series, [12]aneN$_4$, is unusual in that the ligand folds to give cis coordination because the metal ion is too large to allow a planar

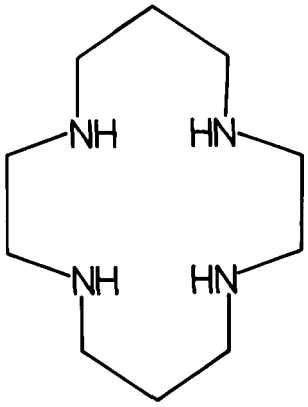

[14]aneN$_4$

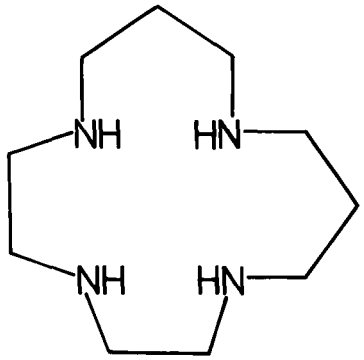

iso[14]aneN$_4$

6

arrangement, explaining the EPR parameters for this species (*73*). Stability constants for addition of anions to nickel(III) planar macrocyclic complexes have been determined (*75, 77–80*), as shown in Table IV, and the kinetics and mechanisms of substitution reported (*75*).

In confirmation of the EPR studies, the X-ray structures of the complexes [Ni^{III}[14]aneN$_4$(Cl)$_2$]Cl (*81*) (Fig. 4) and [Ni^{III}[14]aneN$_4$(NCS)$_2$] (*82*) show a tetragonally elongated geometry. For the former complex, equatorial Ni–N bond lengths are 1.970 Å, shorter than the 2.058 Å found for the corresponding nickel(II) species (*83*). The axial Ni–Cl bonds are also shorter but by a smaller amount. However, bond lengths

TABLE IV

STABILITY CONSTANTS FOR FORMATION OF NICKEL(III) ADDUCTS

Reaction	Medium (moles/liter)	K	Reference
[Ni^{III}[14]aneN$_4$]$^{3+}$ + Cl$^-$	1.0, 25°C	210 M^{-1}	*75*
[Ni^{III}[14]aneN$_4$]$^{3+}$ + Br$^-$	1.0, 25°C	34 M^{-1}	*75*
[Ni^{III}[14]aneN$_4$]$^{3+}$ + SO$_4^{2-}$	0.3, 22°C	5×10^4 M^{-1}	*77*
[Ni^{III}[14]aneN$_4$]$^{3+}$ + SO$_4^{2-}$	0.3, 22°C	3×10^3 M^{-1}	*77*
[Ni^{III}Me$_6$[14]aneN$_4$]$^{3+}$ + 2SO$_4^{2-}$	0.5, 22°C	5×10^6 M^{-2}	*80*
[Ni^{III}Me$_6$[14]aneN$_4$]$^{3+}$ + 2Cl$^-$	0.3, 22°C	250 M^{-2}	*80*
[Ni^{III}Me$_6$[14]aneN$_4$]$^{3+}$ + 2(C$_8$H$_4$O$_4^{2-}$)	0.3, 22°C	$\geq 10^7$ M^{-2}	*80*
[Ni^{III}H$_{-3}$G$_3$a] + NH$_3$	1.0, 25°C	270 M^{-1}	*122*
[Ni^{III}H$_{-3}$G$_4$]$^-$ + NH$_3$	1.0, 25°C	160 M^{-1}	*122*
[Ni^{III}H$_{-3}$G$_3$a] + imidazole	1.0, 25°C	650 M^{-1}	*122*
[Ni^{III}H$_{-3}$G$_3$a] + pyridine	1.0, 25°C	55 M^{-1}	*122*

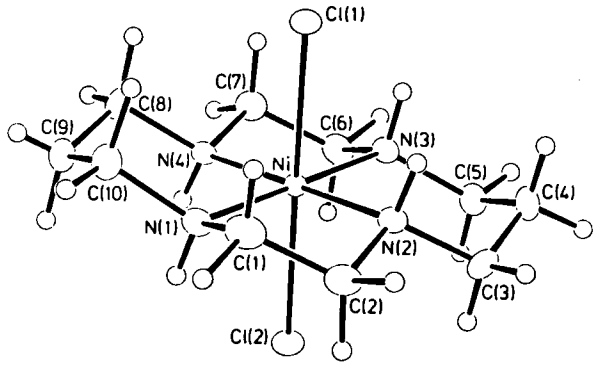

FIG. 4. X-Ray structure of $[Ni^{III}[14]aneN_4(Cl)_2]^+$; from Ref. *81* by permission of the authors and the Japanese Chemical Society.

and angles within the macrocyclic ligand are normal, supporting the concept of metal-centered oxidation.

Substituents on the macrocyclic backbone affect the redox characteristics by restricting axial ligand binding which would stabilize the higher oxidation state (*77–80*). This stabilization is not only thermodynamic but also kinetic in nature. It has been shown (*80*) that decomposition of $[Ni^{III}Me_6[14]aneN_4X_2]^{(3-2n)+}$ in aqueous media containing coordinating anions, X^{n-}, proceeds primarily through the unsubstituted species $[Ni^{III}Me_6[14]aneN_4(H_2O)_2]^{3+}$. The mechanism involves ligand oxidation by proton abstraction and the formation of imine groups. A similar mechanism is proposed for decomposition in acetonitrile (*84*), though some details of the intermediates involved are in dispute. Extensive use of the pulse radiolysis technique has been made to elucidate these species (*85–88*).

In general, unsaturation in a neutral macrocyclic ligand makes oxidation less favorable. Imine donors are less capable of stabilizing the higher oxidation states, particularly when they are in conjugation. However, dianionic deprotonated diimine donors are readily oxidized at low potentials (*64*) to give the corresponding nickel(III) complexes, which are determined from EPR parameters to be square–planar. This is most likely due to a strong π bonding interaction in which the metal ion d_{z^2} orbital is stabilized such that the unpaired electron is removed from a d_{xy} orbital. Deprotonation phenomena have been studied (*89, 90*) with related complexes and, surprisingly, the pK_a of the nickel(III) complex exceeds that of nickel(II), possibly as a result of coordination number changes. The deprotonated form decomposes through a ligand radical which readily dimerizes (*91*).

The ease of formation of higher oxidation-state nickel complexes with oligopeptide ligands has prompted incorporation of amide donors into the macrocyclic framework (*92–98*). Dioxo derivatives of the tetraaza macrocycles in which there are two amine and two deprotonated amide (imide) donors stabilize tetragonally elongated nickel(III) complexes in aqueous media. In the presence of coordinating anions such as sulfate, reduction potentials are somewhat higher than those of the corresponding saturated tetraaza macrocycles (*92, 96*), a consequence of weaker axial ligand binding which stabilizes the higher oxidation states. However, in the presence of poorly coordinating anions, the order of the potentials is reversed (*95*). Somewhat surprisingly, the small, 12-membered macrocycle (*97, 98*) has the lowest reduction potential of those represented.

The thermodynamic and kinetic stabilization of nickel(III) macrocyclic complexes by axial coordination has prompted a number of new approaches. Studies with tetraaza macrocyclic ligands with pendant donors acting as potential fifth ligands have had some success (*96, 99, 100*). Oxidation of $[Ni^{II}[14]aneN_4CH_2CH_2py]^{2+}$ in aqueous solution

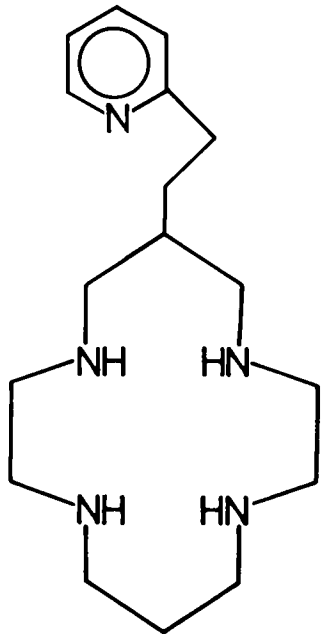

$[14]aneN_4CH_2CH_2py$

7

yields EPR evidence for axial coordination of the pyridine nitrogen, which appears to have little effect on the reduction potential. This may be the result of comparable axial coordination of both oxidation states of the complex; however, reduction potentials were measured in sulfate media, known to stabilize the higher oxidation state, so that this apparent lack of stabilization is misleading. In the case of the corresponding bis oxo complex $[Ni^{III}H_{-2}[14]dioxoaneN_4CH_2CH_2py]^+$ in which H_{-2} indicates deprotonation at both amide nitrogens, there is

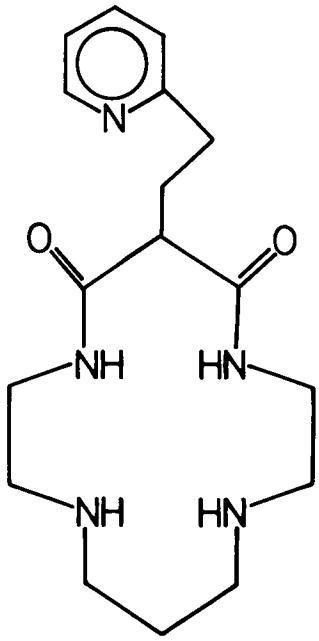

$[14]dioxoaneN_4CH_2CH_2py$

8

no evidence for axial coordination. Only for the 13-membered species with a pendant pyridine N oxide is there a significant decrease in reduction potentials (*96*).

The situation with pendant phenol groups is much less ambiguous. The crystal structure of the nickel(II) complex $[Ni^{II}H_{-1}[14]ane-N_4C_6H_5OH]^+$ (Fig. 5) shows it to be a square–pyramidal, high-spin species and the reduction potential of the nickel(III) complex is 0.15 V lower than that of the parent saturated 14-membered macrocyclic complex (*100*). Strong coordination by phenolate oxygen is even more

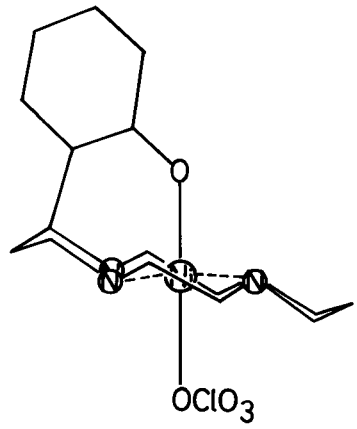

FIG. 5. X-Ray structure of $[Ni^{III}H_{-1}[14]aneN_4C_6H_5OH(ClO_4)]$; from Ref. *100* by permission of the authors and the American Chemical Society.

dramatically shown in the complex $[Ni^{II}H_{-1}[13]aneN_4C_6H_5OH]^+$, where deprotonation of the phenol group combined with the smaller ring size changes the ligand geometry from a square–planar low-spin species with planar tetraaza coordination to a high-spin six-coordinate species in which the macrocycle is bound in folded form (*99*).

A second approach to provide axial coordination with macrocyclic ligands has been the use of pentaaza and hexaaza macrocyclic ligands wherein the fifth and sixth ring nitrogens may be available for axial binding (*101*). Use of the saturated pentaaza macrocycles [15]aneN$_5$, [16]aneN$_5$, and [17]aneN$_5$ gives no dramatic stabilization of the higher oxidation state (*72, 73*). Reduction potentials of the nickel(III) complexes are more positive than for $[Ni^{III}[14]aneN_4]^{3+}$, although the values have been measured in a medium (CH_3CN) where axial stabilization of tetragonal nickel(III) has been established, masking the desired effect. In aqueous media, the oxo macrocycles show lower potentials (*102*). The species $[Ni^{II}H_{-2}[16]dioxoaneN_5]$ is high spin, five coordinate with two imine and two amine nitrogen donors in the equatorial plane and the fifth ring nitrogen coordinated axially (*103*). The angle between the perpendicular to the N_4 plane and the axially coordinated nitrogen decreases from 18.4 to 7.7° on oxidation from nickel(II) to nickel(III) as a result of a contraction in the planar Ni–N bond lengths (*104*). These 16-membered dioxopentaaza macrocyclic complexes have been shown to activate molecular O_2 in the oxidation of benzene to phenol (*102, 105*). It is proposed that this takes place by formation of an adduct with O_2, for which there is

some evidence, the most convincing being the appearance of additional hyperfine coupling in the nickel(III) EPR spectrum when $^{17}O_2$ is present compared with $^{16}O_2$ (*102*).

The six-membered macrocycle [18]aneN_6 forms a high-spin six-coordinate complex with nickel(II) which can be oxidized in acetonitrile solution to give a paramagnetic nickel(III) complex with an axial EPR spectrum indicating a tetragonally compressed octahedral geometry (*73*). Six-coordinate geometry is also possible with formation of bis complexes with the triaza macrocycle [9]aneN_3, and these remarkable species have attracted much interest (*106, 107*). The small nine-membered macrocycle forms a nickel(III) complex more thermodynamically stable than either [10]aneN_3 or [11]aneN_3 (*108*). The crystal structure reveals (*33*) a distorted octahedron in which two triaza macrocyclic ligands are coordinated facially and the Ni–N bond lengths are in two groups, four with the short distance of 1.971 Å and two with 2.110 Å, comparable with the Ni–N distance in the corresponding octahedral nickel(II) complex (*109*). Although the *X*-band EPR of frozen glasses of the complex yield spectra which are interpreted as rhombic, detailed *Q*-band studies reveal a spectrum consistent with the X-ray structure (*33*).

3. Amino Acids and Peptides

There are reports of transient nickel(III) complexes formed in pulse radiolysis experiments with high-spin nickel(II) in glycine solutions (*21*), but oligopeptide complexes containing deprotonated peptide linkages provide a much more extensive chemistry and have been examined in greater detail. At pH > 8, oligopeptide ligands, such as tetraglycine G_4, form low-spin diamagnetic, square-planar complexes with nickel(II) in which peptide hydrogens are ionized from the coordinated groups (*110*). The resulting complex (*111*)$[Ni^{II}H_{-3}G_4]^{2-}$ is inert to substitution, with a rate constant for cleavage of the terminal Ni–N bond of 1.6×10^{-5} sec^{-1} at 25°C.

The observation (*112–115*) that neutral aqueous solutions of $[Ni^{II}H_{-3}G_4]^{2-}$ consume molecular oxygen with the appearance of a strongly absorbing transient at 350 nm lead to detailed investigations and discovery of nickel(III)–peptide complexes (*113*). The oxidized nickel complexes have absorption maxima around 325 and 240 nm ($\varepsilon = 5240$ and $\sim 11{,}000$ M^{-1} cm^{-1}, respectively for $[Ni^{III}H_{-3}G_4]^-$). Reduction potentials (*116*) (Table II), measured by cyclic voltammetry, show a small dependence on ligand structure which can be correlated

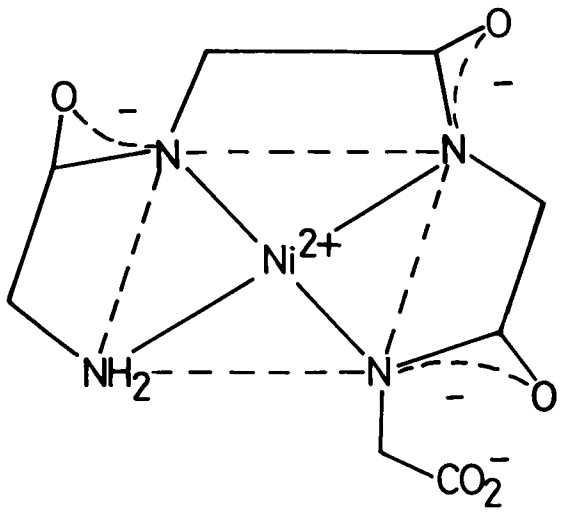

$[Ni^{II}H_{-3}G_4]^{2-}$

9

with the equatorial ligand-field stabilization energy. However, the dependence on the ligand field is smaller than expected on the basis of square–planar geometry for the nickel(III) complex and suggests axial coordination of the solvent. Temperature-dependence studies (*117*) reveal a positive entropy change for the reduction of 15 cal K^{-1} mol^{-1} corresponding to the release of two water molecules.

$$[Ni^{III}H_{-3}G_4(H_2O)_2]^- + e \rightleftharpoons [Ni^{II}H_{-3}G_4]^{2-} + 2H_2O \qquad (2)$$

Tetragonally elongated geometry is confirmed from EPR measurements (*118–121*) and there is a trend in the g values (*118*) with an increasing orbital contribution in the order $N^- > —NH_2 > —Im \sim CO_2^-$, reflecting the donor strength of the groups. Addition of ligands which bind axially to the complexes can be monitored by the hyperfine interaction (Fig. 6), or by the effect on the reduction potentials of the complexes (*122*) (Fig. 7), allowing evaluation of stability constants (Table IV). The rates of axial substitution are fast, $>4 \times 10^6$ sec^{-1} for the reaction of imidazole with $[Ni^{III}H_{-2}Aib_3]$, faster than comparable reactions with macrocyclic complexes due to the stronger in-plane ligand field.

Axial substitution has both a thermodynamic and a kinetic effect in stabilizing the trivalent complex. In the presence of an excess of the oligopeptide ligands, long-lived bis complexes form (*118*). Reaction of

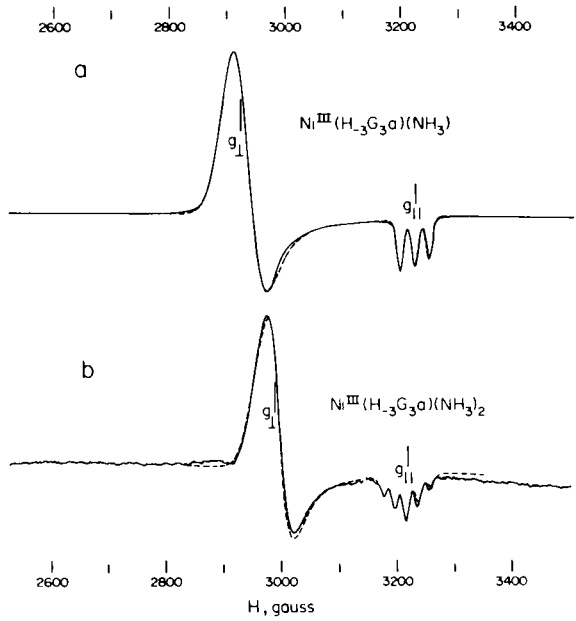

FIG. 6. EPR spectra of (a) $[Ni^{III}H_{-3}G_3a(NH_3)]$ and (b) $[Ni^{III}H_{-3}G_3a(NH_3)_2]$ in aqueous glasses at 100 K; from Ref. *118* by permission of the authors and the American Chemical Society.

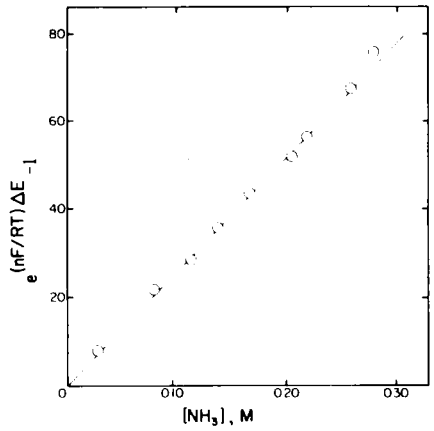

FIG. 7. Plot of $\exp[\Delta E(nF/RT)] - 1$ versus NH_3 for the interaction of $[Ni^{III}H_{-3}G_3a]$ with NH_3; from Ref. *117* by permission of the authors and the American Chemical Society.

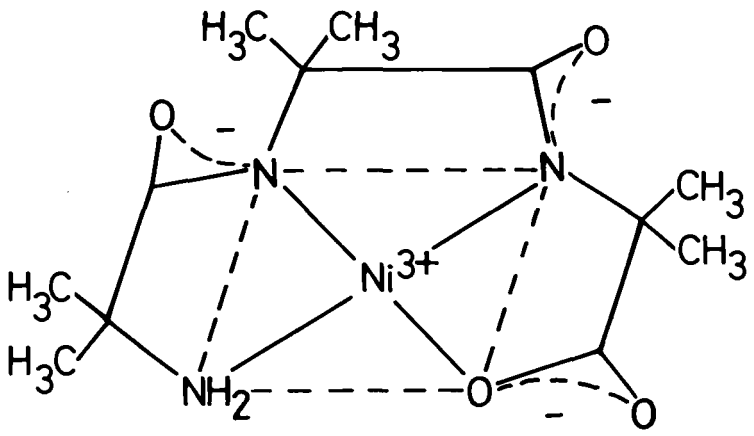

$[Ni^{III}H_{-2}Aib_3]$

10

$[Ni^{III}H_{-2}G_3]$ with excess ligand G_3^- leads (*123*) rapidly to the formation of $[Ni^{III}(H_{-2}G_3)(H_{-1}G_3)]^{2-}$, a tetragonal species with $g_{xx} = g_{yy} > g_{zz}$ and five nitrogens coordinated. Above pH 11 the six-coordinate complex $[Ni^{III}(H_{-2}G_3)_2]^{3-}$ is detected. Thermodynamic arguments suggest that this complex has a reduction potential less than 0.24 V. The tridentate ligand diglycine forms a high-spin six-coordinate nickel(II) complex with two trans deprotonated peptide groups (*111*) that can be oxidized to the corresponding nickel(III) species in which the unique axis contains both deprotonated peptide nitrogens in a compressed tetragonal geometry (*124*). The complex is violet-black in color with an absorption maximum in the visible region at 560 nm. On acidification, the carboxylate groups are protonated and the complex rearranges to give a yellow tetragonal species with two amine and two deprotonated peptide ligands in a plane.

Acid treatment (*125*) of $[Ni^{III}H_{-3}G_4(H_2O)_2]^-$ results in cleavage of the terminal Ni–N deprotonated peptide bond with a rate constant of 0.2 sec^{-1} at 25°C, faster than the corresponding rate for $[Ni^{II}H_{-3}G_4]^{2-}$ Further dissociation of the tridentate tetraglycine ligand is much slower and the intermediate can be trapped by the addition of terpy to give a stable, six-coordinate nickel(III) mixed-ligand complex (*126*). It is notable that the calculated reduction potential for the mixed complex is lower than for either $[Ni^{III}H_{-3}G_4]^-$ or for $[Ni^{III}(terpy)_2]^{3+}$.

The sexidentate amino acid $edta^{4-}$ forms a high-spin nickel(II) complex which can be oxidized to a tetragonally compressed nickel(III)

complex (*127–130*) with $g_{zz} = 2.337$ and $g_{xx} = g_{yy} = 2.139$. Though sensitive to O_2, it is relatively long lived. A related amino acid based on the triaza macrocycle 1,4,7-triazacyclononane-*N*,*N'*, *N''*-triacetate (TACNTA) forms a very stable complex with nickel(II) which aerobically oxidized to the pink nickel(III) species in dilute nitric acid (*131*).

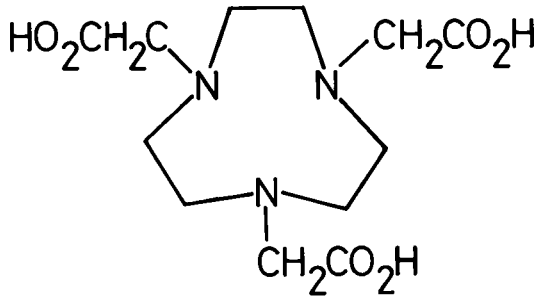

$TACNTAH_3$

11

Metal–nitrogen and metal–oxygen bond lengths in $[Ni^{III}TACNTA]$ are 1.93 and 1.91 Å, respectively, both somewhat shorter than in the corresponding nickel(II) ion.

4. Other Ligands

The earliest high-oxidation-state complex of nickel reported was the heteropoly(molybdate) (*132, 133*) complex $[Ni^{IV}Mo_9O_{32}]^{6-}$, which contains nickel(IV) in an octahedral NiO_6 coordination environment. There is no evidence for the corresponding nickel(III) species but further work on nickel(IV) complexes of this type has been reported recently (*134*). Nickel(III) can be prepared in a six-coordinate oxygen donor environment (*135*) as a tris chelate with 2,2'-bipyridine-1,1'-dioxide ($bpyO_2$). The complex has a rhombic EPR spectrum and a reduction potential of 1.7 V, from which an estimate of the reduction potential of the ion $[Ni^{III}(H_2O)_6]^{3+}$ of 2.5 V (versus nhe) has been calculated.

One recent, important development has been (*136*) the electrolytic preparation from $[Ni^{II}(CN)_4]^{2-}$ of $[Ni^{III}(CN)_4(H_2O)_2]^-$, which has a half-life of 11 minutes in acidic solution at 25°C and serves as a precursor for the incorporation of nickel(III) in other ligand system. The complex is tetragonally elongated from its EPR spectrum and can add other anions axially. The bis aquo species has an absorption

maximum at 225 nm ($\varepsilon = 1.16 \times 10^4\ M^{-1}\ cm^{-1}$) and a reduction potential of 1.19 V (versus nhe).

5. *Remarks on Structural Probes of Higher Oxidation-State Nickel*

It is worthwhile making some comment on the primary data used for characterization of nickel(III) and nickel(IV). Reference to Table I reveals that EPR is an effective probe of nickel(III) structure, but without detailed analysis it gives little indication of the electronic distribution. What is becoming clearer as data on a variety of structures are reported is the finding of both tetragonally elongated and tetragonally compressed geometries for nickel(III), perhaps suggesting that there can be rapid interchange between the two Jahn–Teller distorted forms.

The extensive X-ray data on higher order oxidation state complexes is also worthy of comment. It has already been mentioned that Ni–N(amine) bond lengths for high-spin nickel(II) are in the range 2.1–2.2 Å and for low-spin nickel(II) are 1.9–2.0 Å. For nickel(III) they vary (*33, 80–82, 131*) from 1.93 to 2.11 Å, the large range a function of the Jahn–Teller distortion and the finding that tetragonally elongated structures predominate. On a small sample of nickel(IV) complexes (*51, 52*) the Ni–N(amine) lengths are 1.955 and 2.006 Å, a little larger than might be expected. For the Ni–N(imine) systems examined the situation is more in line with that expected with 2.01–2.09 Å for nickel(II) (*34, 51, 53*), 1.92–2.02 Å for nickel(III) (*32*), and 1.84–1.87 Å for nickel(IV) (*44, 51, 52*). Imide bond lengths are also shorter for nickel(III) (*103*) than for nickel(II) (*103, 111*).

In Table II the reduction potentials of a variety of nickel(III) complexes are reported. The values have been corrected as well as is possible for standard conditions and it is revealing that the potentials, particularly of complexes which have a strong square–planar ligand, show marked variations depending on the donor ability of the solvent and coordinating anions. This has itself evolved into a structural probe (*108, 117*) but clearly it makes comparisons difficult and overinterpretation somewhat dangerous.

B. Kinetic Studies

1. *Complex Formation Reactions of Nickel(III)*

Electrochemical studies (*62, 64, 106, 137*) have shown that nickel(III) complexes with macrocycles, peptides, and diimine ligands are rel-

atively strong oxidants ($E^0 = 0.9-1.3$ V versus nhe), and in acidic solutions many of these species are sufficiently long lived to enable studies of both complex formation and redox reactivity. It has been suggested (*86*) that the role of the ligands is such that not only is the energy of the antibonding orbital [containing the electron to be removed on oxidation from nickel(II)] raised through strong M–N in-plane interactions, but also encapsulation and modification of the ligand pK values reduces the reactions with solvent.

Relatively few studies are available for complex formation reactions of nickel(III) macrocycles. For the tetraaza macrocycles, the octahedral structure of the ion requires that the two axial sites are coordinated by solvent. In aqueous media, reaction of $[Ni^{III}[14]aneN_4(OH_2)_2]^{3+}$ with halide ions may be monitored at $\lambda \sim 320-350$ nm. Owing to the relatively facile hydrolysis and redox decomposition of the nickel(III)–diaquo macrocycles—$[Ni^{III}[14]aneN_4(OH_2)_2]^{3+}$ decomposes within 1 hour at pH 2–3 (and more rapidly with increasing pH)—the early kinetic studies involving nickel(III) were made using pulse radiolysis (*86*) or flash photolysis techniques (*138*). However, the presence of axially coordinated chloride (*75, 80*), sulfate (*79, 80*), or phthalate (*80*) renders the nickel(III) center much more stable kinetically. Pulse radiolysis studies (*86*) of the diaquo-*trans*-($Me_6[14]dieneN_4$)nickel(III), $[Ni^{III}Me_6[14]dieneN_4(H_2O)_2]^{3+}$, with Br^-

$$[Ni^{III}Me_6[14]dieneN_4(H_2O)_2]^{3+} + Br^- \underset{k_b}{\overset{k_f}{\rightleftharpoons}} [Ni^{III}Me_6[14]dieneN_4(H_2O)Br]^{2+} \quad (3)$$

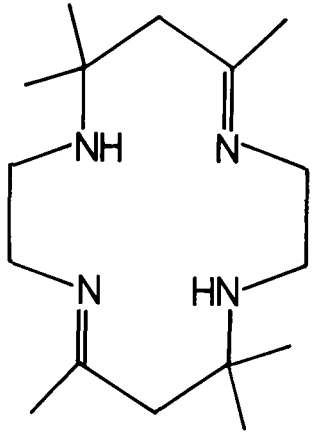

$Me_6[14]dieneN_4$

12

showed that at pH ~3, $k_f \sim 1300\ M^{-1}\ sec^{-1}$ ($I = 0.01\ M$) with $k_b = 120\ sec^{-1}$. The strong oxidizing power of the unsaturated ligand complex (~1.30 V) results in oxidation of the bromide to bromine. In the case of [14]aneN$_4$ (*75*) or its substituted derivatives (*139*) the lower E^0 values (0.96–1.1 V) are such that while formation reactions of stable chloride and bromide species may be monitored, the iodo complexes rapidly undergo redox reactions (*140*).

Rate constants derived from studies at a variety of hydrogen ion concentrations reveal no discernible kinetic effect from this source. Data for formation and dissociation of monohalo complexes are presented in Table V. It may be seen that for forward and reverse substitution processes [Eq. (3)] the rates increase in the order [14]aneN$_4$ < *meso*-Me$_2$[14]aneN$_4$ < *meso*-Et$_2$[14]aneN$_4$ ≪ *rac*-Me$_2$[14]aneN$_4$. All four of these complexes have identical chair conformations in the macrocyclic ring, differing only in the presence at the asymmetric centers of two equatorial methyl (or ethyl) groups in the *meso*-Me$_2$[14]aneN$_4$ and *meso*-Et$_2$[14]aneN$_4$ ligands and one equatorial and one axial methyl group in the *rac*-Me$_2$[14]aneN$_4$ complex. With the exception of the *rac*-Me$_2$[14]aneN$_4$ complex, the formation rates fall within an order of magnitude, suggesting a dissociative character to the reaction. There are no data available on solvent exchange rates of nickel(III). It is considered that the increase in rate for the racemic complex derives from steric crowding on one face of the molecule modifying the reactivity and favoring dissociation in the axial direction. Of interest is the observation that for the monochloro and monobromo complexes, there is a slower, second halide-independent rearrangement to a five-coordinate nickel(III) species ($k \sim 0.4\ sec^{-1}$).

TABLE V

RATES OF FORMATION AND DISSOCIATION OF MONOHALO COMPLEXES OF NICKEL(III) MACROCYCLES[a]

Ligand	Cl^-		Br^-		I^-	
	$10^{-3}\ k_f$ ($M^{-1}\ sec^{-1}$)	k_b (sec^{-1})	$10^{-3}\ k_f$ ($M^{-1}\ sec^{-1}$)	k_b (sec^{-1})	$10^{-3}\ k_f$ ($M^{-1}\ sec^{-1}$)	k_b (sec^{-1})
meso-Me$_2$[14]aneN$_4$	2.2	9.4	0.9	21.8	4.0[a]	—
meso-Et$_2$[14]aneN$_4$	3.1	22	2.8	25.6	9.8[b]	—
rac-Me$_2$[14]aneN$_4$	42	66	>10	≥100	29	0.8
[14]aneN$_4$	—	0.9	4.3	0.21	6.1[b]	3.1
Me$_6$[14]dieneN$_4$	—	—	1.3	120	—	—

[a] From Refs. *86*, *139*, and *140*.

[b] Inner-sphere redox reaction; see text.

Although direct complex formation is observed kinetically (stopped flow) and spectrophotometrically, where X = Br or Cl, the reaction with I^- results in an oxidation of the halide. The reactions are rapid and there is the question of inner- or outer-sphere electron transfer, for the [14]aneN$_4$ complex. However, further studies (*140*) using ligand substituted (dimethyl) complexes reveal that for the *rac*-Me$_2$[14]aneN$_4$ isomer, two processes are observed, $k_f = 2.9 \times 10^4\ M^{-1}\ sec^{-1}$ and a subsequent redox step, $k_{red} = 5.5 \times 10^3\ M^{-1}\ sec^{-1}$, both of which are iodide dependent. The mechanism proposed involves the formation of an octahedral complex which further reacts with a second mole of I^- in the redox step:

$$[Ni^{III}rac\text{-}Me_2[14]aneN_4(OH_2)_2]^{3+} + I^- \underset{k_f,\,k_b}{\rightleftharpoons} [Ni^{III}rac\text{-}Me_2[14]aneN_4(I)(OH_2)]^{2+} \quad (4)$$

$$[Ni^{III}rac\text{-}Me_2[14]aneN_4(I)(OH_2)]^{2+} + I^- \xrightarrow{k_{red}} [Ni^{II}rac\text{-}Me_2[14]aneN_4]^{2+} + I_2^- \quad (5)$$

$$I_2^- + [Ni^{III}rac\text{-}Me_2[14]aneN_4]^{3+} \xrightarrow{fast} [Ni^{II}rac\text{-}Me_2[14]aneN_4]^{2+} + I_2 \quad (6)$$

Further evidence of an inner-sphere mechanism is that the reaction rates appear to be too rapid to adhere to the Marcus correlation observed for other complexes with this anion. Also, the rate constants for the halides fall in the same order for all of X = Cl, Br, and I, suggesting a common initial step.

The rate of formation of the inner-sphere complex [Ni^{III}Me$_6$[14]aneN$_4$SO$_4$]$^+$ has been investigated using pulse radiolysis techniques (*77*). Although there is evidence for hydrolysis (pK 3.7 $\pm$ 0.2) of the diaquonickel(III) complex, substitution by SO_4^{2-} occurs only on the unhydrolyzed ion with $k_f = 1 \times 10^6\ M^{-1}\ sec^{-1}$ ($I = 0.03\ M$). After allowance for outer-sphere ion pairing and ionic strength effects, the formation rate constant at $I = 1.0\ M$ is considered to be in the range $3–5 \times 10^2\ M^{-1}\ sec^{-1}$, which is close to those for the halide complexes, confirming the suggestion of a dissociative interchange mechanism in these substitution processes.

In nickel(III) peptide complexes, there is a strong in-plane field provided by the deprotonated peptide linkages (*117, 118*). Two axially coordinated water molecules are present in the tetragonally distorted complexes which exchange much more rapidly than for the [14]aneN$_4$ species with a substitution rate of constant $>10^6\ M^{-1}\ sec^{-1}$ for the formation of the imidazole complex (*141*). However, except for the terminal peptide group, equatorial substitution is very slow. Substitution and rearrangement (*125*) reactions of these species reveal acid-

induced bond breaking ($k \sim 0.1-15\ \text{sec}^{-1}$) as $[H^+]$ increases in the range 0.004–1.0 *M*. These substitutions are reversible in dilute acidic conditions. Coordination of terpyridyl (*126*) at the two axial and the free equatorial sites in a meridional manner yields complexes ($\log K \sim 12.8$) which are stabilized with respect to self-redox decomposition in basic media.

2. Electron Transfer Reactions of Nickel(III)

a. Reactions of Nickel(II)/(III) Ions with Metal Complexes. Relatively few kinetic studies have been made on the oxidation of nickel(II)species. The reactions of $[Ni^{II}[14]aneN_4]^{2+}$ and its derivatives (*143, 144*) with aquocobalt(III) have been investigated. The mechanism may be described in terms of the following reaction scheme:

$$Co^{3+} + [Ni^{II}[14]aneN_4]^{2+} \xrightarrow{k_1} Co^{2+} + [Ni^{III}[14]aneN_4]^{3+} \quad (7)$$

$$CoOH^{2+} + [Ni^{II}[14]aneN_4]^{2+} \xrightarrow{k_2} Co(II) + [Ni^{III}[14]aneN_4]^{3+} \quad (8)$$

The overall second-order observed rate constant is of the form $k_0 = k_1 + k_2K_h/[H^+]$. Part of the difficulty in assigning the reaction types lies in the square–planar/octahedral equilibrium of the nickel(II) ions. However, Endicott has assigned an outer-sphere mechanism for reaction Eq. (7). Confirmation of this is provided in the reactions of $[Ni^{II}([9]aneN_3)_2]^{2+}$, which retains octahedral geometry (*107*) in both the reduced and oxidized states. A rate law similar to that above is observed (*145*) in the oxidation of a nickel(II) oxime complex by cobalt(III). In this case, the nickel(III) formed is a transient and further reaction takes place to yield a nickel(IV) species. Of interest is the fact that for the $CoOH^{2+}$ pathway with reductants (*107, 145, 146*) which are unambiguously outer sphere, the self-exchange rate constant (vide infra) for the $CoOH^{2+/+}$ couple ($\sim 10\ M^{-1}\ \text{sec}^{-1}$) is about 11 orders of magnitude greater than that for the aquo $Co^{3+/2+}$ system (*143*). Self-exchange data have also been derived from the reactions of nickel(II) macrocycles and oxime complexes with $[Fe(phen)_3]^{3+}$ complexes (*147, 148*).

b. Reactions of Nickel(III) Complexes. The stabilization of this oxidation state by macrocycles, diimines, and oximes has enabled a good deal of kinetic investigation into electron transfer processes involving these ions. Also, in many systems there is little ambiguity regarding the pseudooctahedral nature of the low-spin d^7 ions. These complexes have redox potentials (versus nhe) in the order 0.6–1.3 V (*10,*

106, 108) so that systematic studies on related species permit evaluation of self-exchange rates via a Marcus correlation. Also, as more structural information becomes available it is possible to relate these rate constants with bond extension or contraction leading to the transition state complex.

The oxidations by $[Ni^{III}([9]aneN_3)_2]^{3+}$ and $[Ni^{III}([10]aneN_3)_2]^{3+}$, of a series of metal poly(pyridine) complexes, have been investigated (*107, 146, 149*). A typical reaction of this type is seen in Eq. (9), where

$$[Ni^{III}([9]aneN_3)_2]^{3+} + [Co(phen)_3]^{2+} \longrightarrow [Ni^{II}([9]aneN_3)_2]^{2+} + [Co(phen)_3]^{3+} \quad (9)$$

the second-order rate constant $k_{12} = 5.6 \times 10^5\ M^{-1}\ sec^{-1}$. There are no hydrogen ion effects on this outer-sphere reaction. The rate law and lack of $[H^+]$ dependence are a feature of these processes, which are particularly suitable for the calculation of rate constants, since no bond making or breaking occurs during electron transfer. As a result of the redox reaction, the coordination shells and immediate environments of the reactants and products will change. Using cross-reaction data of the type in Eq. (9), the rate constant for reaction, k_{12}, is related (*150–152*) to the individual self-exchange reaction rates k_{11}, k_{22} and to the overall equilibrium constant, K_{12}, by the expression, Eq. (10).

$$k_{12} = (k_{11}k_{22}K_{12}f_{12})^{1/2}W_{12} \quad (10)$$

where

$$\ln f_{12} = \frac{[\ln K_{12} + (W_{12} - W_{21})/RT]^2}{4\left[\ln\left(\frac{k_{11}k_{22}}{A_{11}A_{22}}\right) + \frac{W_{11} + W_{22}}{RT}\right]}$$

$$W_{12} = \exp[-(w_{12} + w_{21} - w_{11} - w_{22})/2RT] \quad (11)$$

$$w_{ij} = \frac{Z_iZ_je^2}{D_s\sigma_{ij}(1 + \beta\sigma_{ij})} \quad (12)$$

$$A_{ii} = \left[\frac{4\pi Ne^2\nu\beta\gamma r}{1000}\right]_{ii} \quad (13)$$

where w_{ij} represents the work required to bring together ions i and j ofcharges Z_iZ_j to the separation distance $\sigma_{ij} = r_i + r_j$ and $\beta = (8\pi Ne^2/1000D_skT)^{1/2}$. The nuclear vibration frequency which destroys

the activated complex configuration is designated $v\beta$ and γr is the thickness of the reaction layer. A value of 3×10^{10} M^{-1} Å^{-1} sec^{-1} has been quoted for the value of A/σ^2.

A plot of $\ln k_{12} - \ln w_{12}$ against $\ln(k_{22}K_{12}f_{12})$ should be linear with slope of 0.5 and intercept corresponding to $\frac{1}{2}\ln k_{11}$, where k_{11} is the self-exchange rate for the nickel(III)/(II) couple. Relatively few direct measurements have been made of the self-exchange in nickel(III/II) systems. The fact that the nickel(III) complexes, being low-spin d^7, are ESR active has permitted an estimate (*148*) of the exchange between $[Ni^{III/II}[14]aneN_4]^{3+/2+}$ complexes. Using ^{61}Ni-($I = 3/2$) where a quartet feature observed in g_{zz} is consistent with hyperfine interaction between the unpaired electron and the ^{61}Ni nucleus, the reaction proceeds with enhancement of the quartet (Fig. 8).

$$[^{58}Ni^{III}[14]aneN_4]^{3+} + [^{61}Ni^{II}[14]aneN_4]^{2+} \rightleftharpoons [^{58}Ni^{II}[14]aneN_4]^{2+} + [^{61}Ni^{III}[14]aneN_4]^{3+} \quad (14)$$

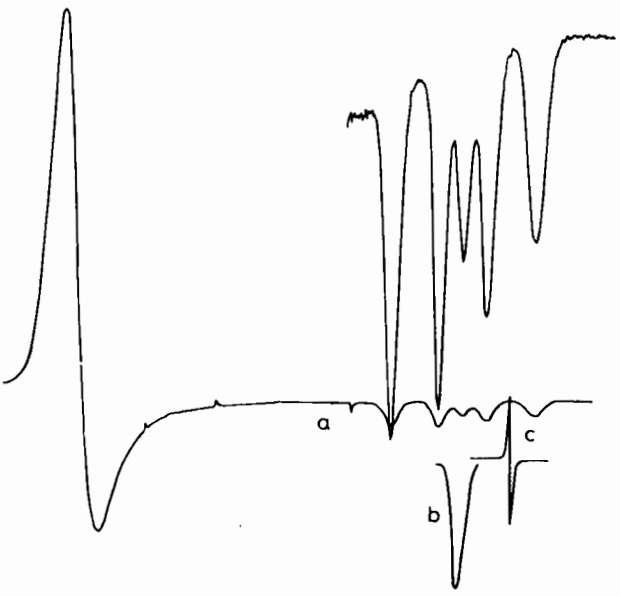

FIG. 8. (a) The EPR spectrum of $[^{61}Ni^{III}[14]aneN_4(SO_4)_2]^-$ and the corresponding spectra of (b) the ^{58}Ni complex and (c) dpph; from Ref. *148* by permission of the authors and the Royal Society of Chemistry.

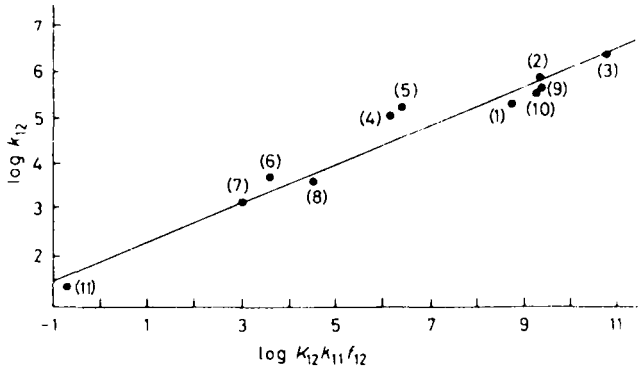

FIG. 9. Plot of $\log k_{12}$ against $\log K_{12}k_{11}f_{12}$; from Ref. *149* by permission of the authors and the Royal Society of Chemistry.

Monitoring of g_{zz} with time affords an approximate value for k_{11} ($\sim 1 \times 10^3\ M^{-1}\ \text{sec}^{-1}$). Substantiation of this value was obtained in independent cross-reactions between $[Ni^{II}[14]aneN_4]^{2+}$ and $[Fe(phen)_3]^{3+}$. As mentioned previously, for the nickel[14]aneN$_4$ species the question of solvation in the axial positions is not completely resolved. By using $[Ni^{III/II}([9]aneN_3)_2]^{3+/2+}$ and the corresponding 10-membered ring complex, where octahedral geometry is retained, excellent cross-correlations have been obtained (Fig. 9), leading to calculated self-exchange rates. A feature of several of the reactions is the closely similar reduction potentials leading to an equilibrium condition,

$$[Ni^{III}([9]aneN_3)_2]^{3+} + [Ni^{II}[14]aneN_4]^{2+} \rightleftharpoons [Ni^{II}([9]aneN_3)_2]^{2+} + [Ni^{III}[14]aneN_4]^{3+} \quad (15)$$

where $\Delta E = 0.05$ V. In such circumstances, suitable manipulation of the reagent concentrations permits both the forward and back reactions to be treated as pseudo first order. The observed rate constant k_{obs} may then be expressed in the form (*149*) $k_{obs} = k_f\{[Ni^{II}[14]aneN_4]^{2+}\} + k_b\{[Ni^{II}([9]aneN_3)_2]^{2+}\}$. At constant $[Ni([9]aneN_3)_2]^{2+}$ concentration, the plot of k_{obs} against $[Ni^{II}[14]aneN_4]^{2+}$ concentration should be linear, and the intercepts obtained under differing concentrations are a linear function of $[Ni([9]aneN_3)_2]^{2+}$. From these data, both k_f and k_b may be derived (Fig. 10).

Several isomers of $[Ni^{II}Me_2[14]aneN_4]^{2+}$, and one of $[Ni^{II}Et_2[14]aneN_4]^{2+}$, have been isolated (*153*). Using crystallography and ^{13}C

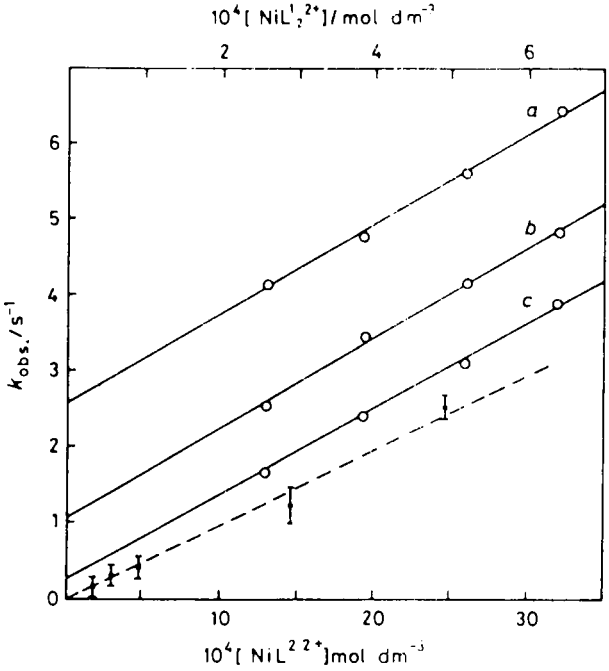

FIG. 10. Plots of k_{obs} against $[NiL']^{2+}$ at various concentrations (a–c) of $[NiL^2]^{2+}$. The dashed line represents the dependence of $[NiL^2]^{2+}$; from Ref. *149* by permission of the authors and the American Chemical Society.

and ^1H NMR spectroscopy, the α-$[Ni^{II}$*meso*-$Me_2[14]aneN_4]^{2+}$ and $[Ni^{II}$*meso*-$Et_2[14]aneN_4]^{2+}$ species, derived from the meso forms of the dimethyl and diethyl ligands, have equatorial distribution of the

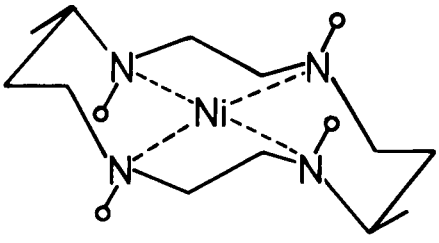

α-$[Ni^{II}$*meso*-$Me_2[14]aneN_4]^{2+}$

13

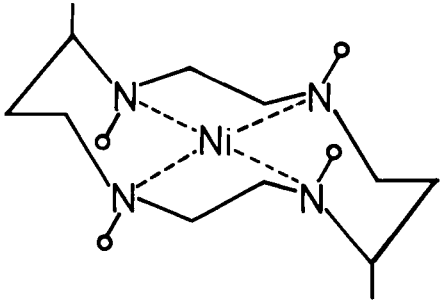

β-$[Ni^{II}$*meso*-$Me_2[14]aneN_4]^{2+}$

14

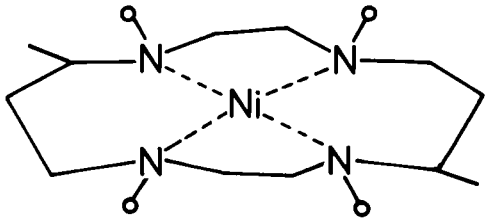

δ-[Ni^{II}*meso*-Me_2[14]aneN_4]$^{2+}$

15

substituent groups, leaving the nickel(II) center readily available for solvation. In the case of the β-[Ni^{II}*meso*-Me_2[14]aneN_4]$^{2+}$, axial configurations of the methyl groups are indicated. In δ-[Ni^{II}*meso*-Me_2[14]aneN_4]$^{2+}$, there is a modification of the 14-membered ring system to the *trans*-IV structure. Details of the stereochemistry of the ring conformation are presented in Table VI. Significant differences are observed in the solution and redox properties for the various isomers. As is known, nickel(II) macrocycles exhibit a square–planar octahedral equilibrium (K_{eq}) with water (solvent) ligating in the axial positions of the six-coordinate ion. This is accompanied by a marked decrease in the absorbance at ~450 nm. Approximate values of K_{eq} may be derived from changes in the extinction coefficient. Fabbrizzi (*68*) has previously obtained a value of $K_{eq} = 0.39$ for the parent [14]aneN_4 (Table III). The values of ~0.4 and ~0.7 for the equatorially disposed dimethyl and diethyl groups suggest the same degree of unhindered approach of the axial solvent. However, for the β isomer, significant

TABLE VI

RING CONFORMATION, SOLUTION, AND REDOX PROPERTIES OF NICKEL(II) DERIVATIVES OF [14]aneN_4

Complex	k_{eq} [a]	Substituent[b]	E^{0} [c]	Ring conformation	Configuration
α-*meso*-Me_2[14]aneN_4	0.4	eq, eq	0.995	trans III	*S,S,R,R*
meso-Et_2[14]aneN_4	0.4	eq, eq	0.990	trans III	*S,S,R,R*
β-*meso*-Me_2[14]aneN_4	<0.05	ax, ax	1.155	trans III	*S,S,R,R*
δ-*meso*-Me_2[14]aneN_4	<0.05	int, int	1.145	trans IV	*S,R,R,S*
rac-Me_2[14]aneN_4	0.2	int, ax	1.115	trans III	*S,S,R,R*

[a] Equilibrium in 0.5 $HClO_4$.

[b] eq, Equatorial; ax, axial; int, intermediate.

[c] Voltage versus a normal hydrogen electrode.

steric hindrance is anticipated, owing to the axial orientation of the ring substituents. In this instance, there is a marked decrease in the value of K_{eq}. A similar low value is found for the δ isomer, which has a *trans*-IV structure with groups intermediate between axial and equatorial. The ability of the ring to fold has been considered as a factor in the formation of reaction intermediates (*154, 155*) and this may be a feature in these systems. Of equal interest are the pronounced changes in the redox potentials of the nickel(III)/(II) couples (Table VI). Again, the E^0 values for the equatorially substituted species are similar to the $[Ni^{III/II}[14]aneN_4]^{3+/3+}$ value. However, increased strain in the system leads to more strongly oxidizing species. Using the outer-sphere reagent $[Ni^{II}([9]aneN_3)_2]^{2+}$ as reductant, a series of cross-reactions with these and other macrocycles was studied. Pronounced variations are observed (Table VII) in the rates of self-exchange for the various isomers. By examining the inner- and outer-shell reorganizational barriers, it is seen that although solvation effects must be included, inner coordination sphere reorganization is important and indeed accounts for the large variations in self-exchange rate constants. This effect is also observed in reactions of the hexamethyl derivatives where the additional methyl groups present increase the barrier to axial solvation. Again significantly lower self-exchange rates are observed. These are shown in Table VII, which lists all the self-exchange data so far derived for nickel(II)/(III) couples.

Reactions of nickel(III) complexes have also been used to examine exchange parameters for other metal ion complexes. An excellent correlation is provided in a Marcus treatment of the data for the reactions with $TiOH^{2+}$ as reductant (*156*). The self-exchange rate ($TiOH^{2+/+} = 9 \times 10^3\ M^{-1}\ sec^{-1}$) is in excellent agreement with that derived by Sutin (*157*). A feature of this study is that the reaction rates for $[Ni^{III}[14]aneN_4(Cl)_2]^+$ and its dimethyl derivative with $TiOH^{2+}$ are $\sim 10^2$ faster than substitution at the metal center and so the reactions are postulated as outer sphere. Only in conditions of high ($>0.5\ M$) chloride is the axial substitution complete. From the data, the rate constants for the nickel(III)/(II) self-exchanges may be evaluated as 3.4×10^4 and $9.5 \times 10^4\ M^{-1}\ sec^{-1}$, respectively. These values are higher than for other nickel(III) species and may reflect the effects of the lower overall charges on the ions. Also, the nickel(II)/(III) exchange involves transfer of a $\sigma^* d$ electron between a high-spin nickel(II) (d^8) and a low-spin (d^7) nickel(III). X-ray crystal data are available for the oxidized (*81*) and reduced (*83*) forms of the nickel complex. Whereas there is a bond length change of 0.088 Å in the Ni–N equatorial plane, the Ni–Cl differences show $\Delta d = 0.04$ Å.

TABLE VII

SELF-EXCHANGE RATE CONSTANTS FOR NICKEL(III)/(II) COMPLEX

Oxidant	k_{11} (M^{-1} sec^{-1})	Reference
$[Ni^{III}Me_2[14]aneN_4(Cl)_2]^+$	9.5×10^4	*156*
$[Ni^{III}([10]aneN_3)_2]^{3+}$	2.5×10^4	*146*
$[Ni^{III}[14]aneN_4(Cl)_2]^+$	3.4×10^4	*156*
$[Ni^{III}Et_2[14]aneN_4(OH_2)_2]^{3+}$	2.5×10^4	*153*
$[Ni^{III}\alpha\text{-}meso\text{-}Me_2[14]aneN_4(OH_2)_2]^{3+}$	7.5×10^3	*153*
$[Ni^{III}([9]aneN_3)_2]^{3+}$	6×10^3	*149*
$[Ni^{III}Me_2[14]dieneN_4]^{3+}$	3×10^3	*143*
$[Ni^{III}(bpy)_3]^{3+}$	1.5×10^3	*159*[a]
$[Ni^{III}[14]aneN_4(H_2O)]^{3+}$	1×10^3	*148*
$[Ni^{III}rac\text{-}Me_2[14]aneN_4(H_2O)]^{3+}$	1.55×10^2	*153*
$[Ni^{III}Me_6[14]aneN_4(H_2O)]^{3+}$	31	—[b]
$[Ni^{III}\delta\text{-}meso\text{-}Me_2[14]aneN_4(H_2O)_2]^{3+}$	26	*153*
$[Ni^{III}\beta\text{-}meso\text{-}Me_2[14]aneN_4(H_2O)_2]^{3+}$	6	*153*
$[Ni^{III}meso\text{-}Me_6[14]aneN_4(H_2O)_2]^{3+}$	2	*143*
$[Ni^{III}Me_2L]^+$	2×10^3	*163*
$[Ni^{III}Me_2LH]^{2+}$	4×10^2	*163*
$[Ni^{III}Me_4[14]tetraeneN_4(H_2O)_2]^{3+}$	0.009	—[c]
$[Ni^{III}trans\text{-}Me_6[14]dieneN_4(H_2O)_2]^{3+}$	0.009	—[c]
$[Ni^{III}cis\text{-}Me_6[14]dieneN_4(H_2O)_2]^{3+}$	0.008	—[c]
$[Ni^{III}H_{-3}G_3a(H_2O)_2]$	1.2×10^5	*165*[d]
$[Ni^{III}H_{-3}G_4(H_2O)_2]^-$	1.3×10^4	*165*[d]
$[Ni^{III}H_{-3}G_5(H_2O)_2]^-$	4.2×10^4	*165*[d]

[a] McAuley, A., and Olubuyide, O., unpublished data; reaction with $[Ru(bpy)_3]^{3+}$.

[b] Other tris(diimine) complexes react similarly.

[c] Fairbank, M., and McAuley, A., unpublished data; reaction with $[Ni^{III}([9]aneN_3)_2]^{3+}$.

[d] Additional data available in Refs. *164* and *165*.

The relatively small bond length changes in the axial positions may account for the increased rate of electron exchange.

Applications of the Marcus theory to reactions of nickel(III) species with Fe^{2+} and VO^{2+} aquo ions (*158*) lead to values of 10^{-3}–10^{-2} M^{-1} sec^{-1} for $Fe^{3+/2+}$ and 10–10^3 M^{-1} sec^{-1} for $VO(OH)^{2+/+}$. These rate constants are larger than for the corresponding data derived using poly (pyridine) derivatives where there may be a contribution from the π^*–π^* interaction of the ligand orbitals.

As has been noted (*29, 31*), nickel(III) poly(pyridine) complexes may be prepared. Electron-exchange rates have been determined (*15*) from a series of cross-reactions. The rate of the electron transfer reaction has

$$[Ni^{III}(bipy)_3]^{3+} + [Ni^{II}(phen)_3]^{2+} \underset{k_y}{\overset{k_x}{\rightleftharpoons}} [Ni^{III}(bipy)_3]^{2+} + [Ni^{III}(phen)_3]^{3+} \quad (16)$$

been measured in 1.0 M H_2SO_4 in both directions ($K = 0.54$). Because of the similarities of the two species in terms of size and free energy, the values of k_x and k_y (1.1. $\times 10^3$ and 2.0 $\times 10^3$ M^{-1} sec^{-1}) have been used in the expression $k_{11} = (k_x k_y)^{1/2}$, yielding a self-exchange rate constant $k_{11} = 1.5 \times 10^3$ M^{-1} sec^{-1}. Other exchange rates are closely similar to this value. Although crystal-structure data are available for the $[Ni^{III/II}(bipy)_3]^{3+/2+}$ couples, the evidence in terms of geometry is still the subject of discussion. Frozen solution EPR spectra (*31*) of the low-spin d^7 $[Ni^{III}(bipy)_3]^{3+}$ are consistent with tetragonal elongation in the Jahn–Teller distorted system. However, the crystal structure (*32*) at 160 K shows tetragonal compression with two pairs of shorter axial bonds leading to an average difference Δd_0 in the Ni–N bond lengths of 0.12 Å. There is the possibility of a static or dynamic (*33*) disorder where the four longer spacings are the mean of two shorter and two longer bonds. The $\Delta d_0 \sim 0.1$ Å accounts for the relatively slow transfer ($k_{11} = 1.5 \times 10^3$ M^{-1} sec^{-1}) of a $\sigma^* d$ electron when compared to the d^8/d^7 $[Co(bipy)_3]^{+/2+}$ and d^7/d^6 $[Co(bipy)_3]^{2+/3+}$ exchanges. In the former $k_{11} \sim 10^8$ M^{-1} sec^{-1} there is the transfer of a πd electron between high-spin d^8 and high-spin d^7, and there is no significant change in the Co–N bond lengths. This feature and the change in spin multiplicity are responsible for the lower value of $k_{11} \sim 18$ M^{-1} sec^{-1}.

Comparison may now be made of the bond length changes in $[Ni^{III/II}([9]aneN_3)_2]^{3+/2+}$ exchange. The structure of $[Ni^{II}([9]aneN_3)_2]^{2+}$ shows an almost regular octahedron with Ni–N = 2.10 Å (*109*). In the corresponding nickel(III) cation, the six Ni–N bonds form two sets, two at 2.110 Å and four at 1.9711 Å, in keeping with a Jahn–Teller distorted system. Thus the two axial bonds are 0.01 Å longer than in the nickel(II) ion and the four equatorial are shorter by 0.129 Å. The short bonds are very similar to those in $[Ni^{III}(bipy)_3]^{3+}$ (1.924 Å) and in $[Ni^{III}(TACNTA)]$ (1.93 Å) (*131*). In the bis([9]aneN$_3$) system, interligand repulsions are observed in the structure and it is considered that the cavity developed by the two [9]aneN$_3$ ligands is too large for the smaller nickel(III) ion. The single-crystal EPR spectrum is consistent with the unpaired electron in the d_{z^2} orbital. Also, the self-exchange rate constant (6×10^3 M^{-1} sec^{-1}) is similar in magnitude to that for other nickel(III) species [poly(pyridyl) complexes], where bond length changes are of comparable magnitude.

Recent studies by Chakravorty have shown that ligands Me_2LH_2 containing oxime–imine and amine functions can stabilize both

nickel(III) and nickel(IV) oxidation states (*9, 45, 55, 160*). On oxidation, one or more of the oxime protons is lost and if only one oxime group is present (*160*), only nickel(III) is formed. A variety of kinetic studies have been made in which the nickel(III) intermediates have been characterized (*56, 161, 162*). Recently (*163*) the kinetics of the redox equilibrium Eq. (17) have been made as a function of pH. Above pH ~5,

$$[Ni^{IV}Me_2L]^{2+} + [Ni^{II}Me_2L] \rightleftharpoons 2[Ni^{III}Me_2L]^{+} \qquad (17)$$

the reductions of $[Ni^{IV}Me_2L]^{2+}$ by $[Ni^{II}Me_2L]$, $[Ni^{II}Me_2LH]^{+}$, and $[Ni^{II}Me_2LH_2]^{2+}$ take place with second-order rate constants of 1.24×10^6, 3.8×10^3, and 3.5×10^2 M^{-1} sec^{-1}, respectively. Below pH 5, disproportionation of $[Ni^{III}Me_2L]^{+}$ is dominated by the reaction with $[Ni^{III}Me_2LH]^{2+}$ ($k = 3.4 \times 10^3$ M^{-1} sec^{-1}). Protonation of nickel(III) at low pH leads to the reaction $2[Ni^{III}Me_2LH]^{2+} \rightarrow [Ni^{II}Me_2LH_2]^{2+} + [Ni^{IV}Me_2L]^{2+}$ being much slower ($k_2 \sim 4$ M^{-1} sec^{-1}), although this process is favored thermodynamically. The trend in the data may be accounted for, partly by increased charges on the species leading to lower rates. There may also be a change in the electronic structure of the doubly protonated nickel(III) species (*163*). Exchange data derived using a Marcus treatment are presented in Table VII.

Nickel(III) deprotonated peptide complexes are readily prepared by chemical and electrochemical oxidation of the corresponding nickel(II) complex. They are moderately stable in aqueous media (*164*). Electrochemical, EPR, and crystallographic studies are consistent with a low-spin d^7 nickel(III) with tetragonally distorted axial geometry (*154*). Stability constants for axial substitution (*122*) are relatively insensitive to the peptide bound, but show marked deviations (factor of 20) in the order imidazole $> NH_3 \sim N_3^- >$ py. Using the stopped-flow technique, the rate constants for 25 cross-reactions have been determined. For 16 different peptide complexes, the values of the self-exchange rates fall into different groups. For triply deprotonated peptides, $k_{11} = 1.2 \times 10^5$ M^{-1} sec^{-1}, except for the pentaglycine complex $H_{-3}G_5$ (4.2×10^4 M^{-1} sec^{-1}); for doubly deprotonated systems, $k_{11} = 1.3 \times 10^4$ M^{-1} sec^{-1}, except for α-aminoisobutyryl tripeptides (5.5×10^2 M^{-1} sec^{-1}). The reactions studied all have small driving forces ($K_{12} < 50$). Axial binding by Cl^-, Br^-, and N_3^- catalyzes the exchange reactions, but pyridine acts as an inhibitor. In the latter case, there is no opportunity for functioning as a bridging ligand.

The nature of the self-exchange is still under consideration. The planned use of the copper(III)–nickel(II) and (reverse) reactions to

provide information on the nickel(III)/(II) peptide exchange rates showed features such as a marked dependence on the peptide ligand; also, the self-exchange constants derived from the cross-reactions were much larger than outer-sphere nickel(III)/(II) peptide electron transfer data (*166*). It appears that the enhanced pathways may have some inner-sphere character. Steric hindrance of the cross-reactions are important and when bulky ligands are attached to the copper the effect is greater than when associated with the nickel complex.

3. Reactions of Nickel(IV)

The mechanistic chemistry of nickel(IV) is dominated by substitution inert complexes and outer-sphere electron transfer reactions. The diamagnetic $[Ni^{IV}(dmg)_3]^{2-}$ is relatively long lived in aqueous base but unstable below pH 8. At 35°C, the decomposition rate (*37*) is 2.6×10^{-7} sec^{-1}, that of its outside-protonated form $[Ni^{IV}(dmg)_3H]^-$ being 1.16×10^{-5} sec^{-1}. Acid catalysis at lower pH is proposed (*37*) as direct proton transfer to ligand nitrogen, but there is no evidence for general acid catalysis necessary with this mechanism. The nature of the acid-catalyzed decomposition is thought (*167*) to involve ligand oxidation prior to dissociation since species with partially dissociated ligands cannot be trapped with strong nucleophiles, although formation of highly reactive partially dissociated complexes cannot be ruled out. Decomposition is also catalyzed by divalent metal cations (*168*), particularly copper(II) (*169*), which forms a 1:1 adduct with $[Ni^{IV}(dmg)_3]^{2-}$.

Redox reactions involving the nickel(IV) complex are also subject to divalent metal ion catalysis (*170, 171*). Oxidations of the two-electron reductant ascorbate (*40*) and the one-electron reductant $[Fe(CN)_6]^{4-}$ (*172*) have been examined in some detail. Both reactions have as the rate-determining step the transfer of one electron from the reductant to nickel(IV) in an outer-sphere process to give an undetected nickel(III) transient. Spectroscopic properties of the nickel(III) species have been determined by pulse radiolysis (*41*).

Comparisons can be drawn between the chemistry of $[Ni^{IV}(dmg)_3]^{2-}$ and that of the sexidentate bis oxime imine complex $[Ni^{IV}Me_2L]^{2+}$, which is much better characterized from a thermodynamic point of view (*45, 56*). It can be optically resolved (*54*) and shows no indications of protonation above pH 0. The isostructural nickel(III) and nickel(II) complexes are subject to protonation and are much more labile to substitution. Protonation of the oxime–imine chromophore destabilizes the higher oxidation states.

The kinetics and mechanisms of reductions of $[Ni^{IV}Me_2L]^{2+}$ by both one- (*55, 56, 163, 173*) and two-electron (*162, 174, 175*) reagents have been extensively examined. Invariably biphasic behavior is observed with more rapid reduction of nickel(IV) than of the nickel(III) that is produced as a reaction intermediate. The predominant outer-sphere nature allows analysis by Marcus theory and the self-exchange rate for $[Ni^{IV/III}Me_2L]^{2+/+}$ is evaluated (*163*) as 4×10^4 M^{-1} sec^{-1} at 25°C. Attempts to explain this value in terms of Ni–N bond length changes leads to the conclusion that structural changes within the ligand may be important.

The complex $[Ni^{IV}Me_2L]^{2+}$ is significantly more reactive than $[Ni^{IV}(dmg)_3]^{2-}$. For example, in reactions with $[Fe(CN)_6]^{4-}$, the rates are $\geq 10^8$ M^{-1} sec^{-1} (25°C, 0.1 M ionic strength) (*41*) and 0.06 M^{-1} sec^{-1} [35°C, 0.06 M ionic strength (*172*)], respectively. The only other nickel(IV) reagent which has been studied mechanistically in any detail is the 9-molybdonickelate(IV) complex, $[Ni^{IV}Mo_9O_{32}]^{6-}$, with an intermediate rate constant (*176*) of 1.2×10^4 M^{-1} sec^{-1} (25°C, 0.10 M NaCl), although in this case the reaction is very cation dependent. This latter reagent has been used (*177*) in the oxidation of aromatic hydrocarbons and in the decarboxylation of aromatic carboxylic acids in acetic acid media.

V. Reduction of Nickel(II)

A. Coordination Environments and Structural Chemistry

1. Amines and Imines

There is an extensive chemistry of the nickel(I) ion generated by pulse radiolysis which is beyond the scope of this review. Complexes with saturated amines such as 1,2-diaminoethane have been studied by this method and by the γ radiolysis of aqueous glasses, but the species formed have no more than a transient existence. The imine ligands phen and bpy offer a more attractive environment for nickel(I) by allowing electron delocalization over the ligand π system (*178, 179*). A number of complexes of these ligands have been reported in γ-radiolysis studies. The EPR spectra indicate that reduction is primarily metal centered with a significant orbital contribution. Electrochemical reduction of $[Ni^{II}(bpy)_3]^{2+}$ in anhydrous acetonitrile results in $[Ni^{I}(bpy)_3]^{+}$, which can be detected by EPR methods. The reduction potential is reported to be -1.55 V but the complex is thermodynamically unstable with

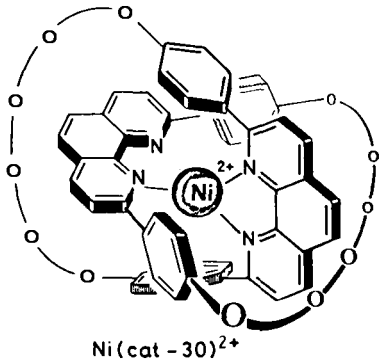

FIG. 11. Structure of nickel(I) catenate; from Ref. *181* by permission of the authors and the Royal Society of Chemistry.

respect to disproportionation (*30, 180*). It has been possible to isolate the bis complex $[Ni^{I}(bpy)_2]ClO_4$, however, indicating that nickel(I) may prefer a lower coordination number with these ligands (*30*). More recently (*181*), a four-coordinate nickel(I) catentate derived from a phenanthroline-based 30-member macrocyclic ring has been reported (Fig. 11). From consideration of the steric requirements of the ligand, a tetrahedral geometry would appear to be favored and this is consistent with the rhombic EPR. The reduced complex has an absorption maximum at 645 nm ($\varepsilon = 2400\ M^{-1}\ cm^{-1}$) and is slow to oxidize in the presence of O_2.

2. Macrocycles

Reduction of a variety of square–planar nickel(II) macrocyclic complexes in acetonitrile leads to the formation of paramagnetic products (*62*). Saturated macrocycle complexes such as $[Ni^{II}[14]aneN_4]^{2+}$ are rather difficult to reduce (*66, 182, 183*), and the products which absorb maximally around 375 nm ($\varepsilon = 26{,}670\ M^{-1}\ cm^{-1}$) are not well characterized from a structural point of view. Methyl substituents on the carbon backbone (*64*) and, more especially, on the ring nitrogen donor atoms (*183*) appear to stabilized the lower oxidation state both thermodynamically and kinetically. Substitution on the ring nitrogens retards ligand dissociation (*183*). Consequently, substituted products have been the subject of more extensive investigations. Reduction potential data are given in Table VIII.

Electrochemical reduction (*64, 184*) of $[Ni^{II}Me_6[14]aneN_4]^{2+}$ gives a product with a well-defined axial EPR signal consistent with nickel(I)

TABLE VIII

SELECTED REDUCTION POTENTIALS FOR NICKEL(II) MACROCYCLIC COMPLEXES

Complex	$E^{0\,a}$		Reference
	CH_3CN	H_2O	
$[Ni^{II}[13]aneN_4]^{2+}$	−1.12	—	*64*
$[Ni^{II}[14]aneN_4]^{2+}$	−1.12	−1.34	*64, 183*
$[Ni^{II}[15]aneN_4]^{2+}$	−0.92	—	*64*
$[Ni^{II}N\text{-}Me_4[14]aneN_4]^{2+}$	—	−0.91	*183*
$[Ni^{II}Me_6[14]aneN_4]^{2+}$	−0.99	−1.18	*64, 183*
$[Ni^{II}N\text{-}Me_4,Me_6[14]aneN_4]^{2+}$	—	−0.74	*183*

[a] Versus a normal hydrogen electrode.

in a tetragonally elongated geometry and an absorption spectrum (*183*) similar to that of the unmethylated complex with a maximum at 380 nm ($\varepsilon = 26{,}320\ M^{-1}\ cm^{-1}$). As with oxidation to nickel(III), the macrocyclic hole size appears to be important in determining the reduction potential (*64, 185*) and as a result of the larger size of the nickel(I) ion, reduction of $[Ni^{II}[16]aneN_4]^{2+}$ is more facile than with the corresponding 15-, 14-, and 13-membered rings. Ligands such as formate ion (*183*) or carbon monoxide (*184, 186*) can bind axially to these nickel(I) species to give adducts which exhibit rhombic EPR spectra and are likely to be five-coordinate.

The nickel(II) macrocycles catalyze the decomposition of alkyl halides (*187, 188*) and the chemistry, which involves nickel–alkyl complexes, has been investigated recently (*189*) in some detail.

Incorporation of one or two imine donors into the macrocyclic framework appears to have little effect on the chemistry of the nickel(I) complexes (*64, 184*) unless the imine groups are in conjugation. However, reduction of $[Ni^{II}Me_4[14]1,3,8,10\text{-tetraene}N_4]^{2+}$ results in an nickel(II)-stabilized ligand radical with $g = 2.008$ rather than a nickel(I) complex (*64, 184*). Addition of a second electron at lower potential is also possible and in the case the product is thought to be a nickel(I)-stabilized ligand radical (*64*). This abrupt change in the nature of the reduced species is not well understood, although clearly the ability of the conjugated diimine system to delocalize electron density over the ligand is an important factor. In one instance (*184, 186*), with a BF_2-containing ring system, both nickel(I)- and nickel(II)-stabilized radical species have been found to be in equilibrium. The proportion of the nickel(I) complex decreases with decreasing temperature.

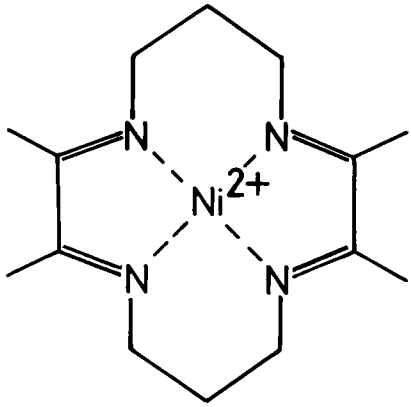

$[Ni^{II}Me_4[14]1,3,8,10\text{-tetraeneN}_4]^{2+}$

16

Addition of π-acceptor ligands which bind axially to the nickel(II)-stabilized radicals induces a change in the electronic configuration. The resulting species are well-defined five-coordinate nickel(I) complexes (*184*, *186*), with $g_{zz} > g_{xx} = g_{yy}$ indicating a tetragonally elongated geometry. Similar results are noted for the one-electron reduced complex formed with the tetraazapyridine–diimine macrocycle (*190*), $[Nicr]^+$, which shows an EPR spectrum corresponding to a

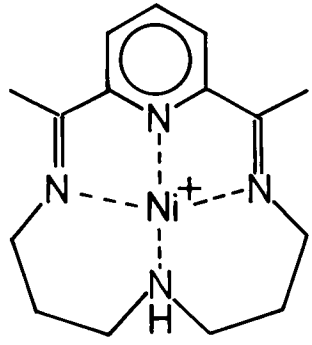

$[Nicr]^+$

17

nickel(II)-stabilized radical in the absence of π-acceptor ligands but a nickel(I) spectrum as a CO, PPh_3, or $P(OMe)_3$ adduct. The correspond-

ing phenanthroline-based pentaaza macrocycle phencr forms (*191*) a pentagonal bipyramidal nickel(II) complex which is reduced to a nickel(I) species exhibiting an axial EPR spectrum with $g = 2.0575$ in acetonitrile solution. In this instance, π-acceptor ligands have a dramatic effect on the reduction potential, stabilizing nickel(I) as a six-coordinate pentagonal pyramid or seven-coordinate pentagonal bipyramid. A second pentaaza macrocycle based on terpy shows similar chemistry (*192*). In this case the nickel(I) complex can be reduced to give a nickel(I)-stabilized radical.

B. Kinetic Studies

Accessibility to the transient nickel(I) species was first gained using e^-_{aq} as reductant in pulse radiolytic experiments (*193*). More recently, Meyerstein (*185*) has shown that ring size effects can be important and that whereas the half-life of $[Ni^{I}[14]aneN_4]^+$ is ~ 2 seconds, that of the nickel(II) ion from [13]aneN$_4$ is of the order of 100 μsec. Several isomeric forms of the tetra-N-methylated (*N*-Me$_4$[14]aneN$_4$) nickel(II) complex ($[Ni^{II}(tmc)]^{2+}$) have been prepared, and a greatly increased stability of the nickel(I) species is seen for the *R,R,S,S* isomer. Electrochemical reduction of $[Ni^{II}(tmc)]^{2+}$ at -1.3 V (versus a standard calomel electrode), in the absence of oxygen, provides stock solutions in the millimolar concentration range which are stable for several hours at 0°C and which may be used for kinetic studies (*189*) (vide infra).

Like other tetraaza metallo(I) complexes, the nickel(I) macrocyclic ions are powerful and labile reducing agents. A point of some interest in these systems is to design a complex couple for which the nickel(I) state is accessible at reasonable potentials. Provided the tetraaza macrocyclic ligand maintains close to planar microsymmetry, reorganizational barriers for a low-spin d^8–d^9 system might be expected to be small (*194*).

Pulse radiolysis studies of nickel(II) tetraaza macrocycles show a marked dependence on ring size. For [13]aneN$_4$, [14]aneN$_4$, and [15]aneN$_4$, the larger radius of the nickel(I) is exhibited in the redox potential and short lifetime of the 13-membered ring. Reductions of $[Ni^{II}[13]aneN_4]^{2+}$ by e^-_{aq} and CO_2^- are close to diffusion controlled in rate. The instability of the reduced ion is considered to be due to the inability of the cation to fit into the ring cavity. Of interest, however, is the reaction [Eq. (18)] in the presence of N_2O (*185*), where the

$$[Ni^{I}[13]aneN_4]^+ + N_2O + 2H_3O^+ \longrightarrow [Ni^{III}[13]aneN_4]^{3+} + N_2 + 3H_2O \quad (18)$$

product is the corresponding nickel(III) complex. Absorption maxima

($\varepsilon \sim 2\text{–}3 \times 10^3\ M^{-1}\ cm^{-1}$) are very similar ($\lambda_{max} = 370$ nm) for all three monovalent nickel species. For the 15-membered ring system, which in the nickel(II) case is virtually exclusively octahedral (*195*), there is no reduction by CO_2^- as is observed for the other low-spin nickel(II) ions. Although thermodynamically allowed, it is concluded that reduction by CO_2^- takes place via a bridged intermediate which is not formed for the high-spin system. However, in the presence of the free radical $CH_2C(Me)_2OH$, it is postulated that a transient alkyl complex is formed which rapidly undergoes hydrolysis under the reaction conditions:

$$\begin{array}{l} [Ni^{I}[15]aneN_4]^+ + \cdot CH_2C(Me)_2OH \longrightarrow [[15]aneN_4NiCH_2C(Me)_2OH] \\ \qquad\qquad\qquad\qquad\qquad\qquad\qquad\qquad\qquad\qquad \Big\downarrow H_2O \\ [[15]aneN_4Ni^{II}(OH_2)_2]^{2+} + CH_2{=}C(Me)_2 \end{array} \qquad (19)$$

Alkylnickel formation has also been extensively studied in the one-electron reductions of alkyl halides and peroxides by a nickel(I) macrocycle (*189, 196, 197*). Although two forms of the nickel(II) isomers of the tetra-N-methylated macrocycle are known, there is no ready interconversion between the $[(R,R,S,S,)Ni^{II}(tmc)]^{2+}$ and $[(R,S,S,R)]Ni^{II}(tmc)]^{2+}$. Solutions of the $[Ni^{I}(tmc)]^+$ complexes can be prepared in alkaline media (*183*), although within several nours isomerization of the nickel(I) forms takes place. The complexes are again strong reductants ($E^0 = -0.90$ V). Using the $1R,4R,8S,11S$ isomer (Fig. 12), Espenson and his co-workers have examined reactions with a variety of primary alkyl halides (*189*). For most systems studied, the overall reactions exhibit the stoichiometry according to Eq. (20):

$$2[Ni^{I}(tmc)]^+ + CH_3I + H_2O \longrightarrow 2[Ni^{II}(tmc)]^{2+} + I^- + CH_4 + OH^- \qquad (20)$$

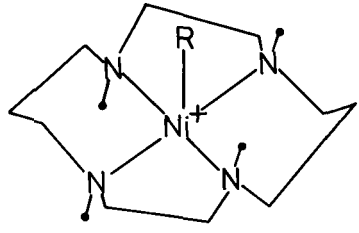

FIG. 12. $[R\text{-}Ni^{I}(R,R,S,S\text{-}tmc)]^+$; from Ref. *189* by permission of the authors and the American Chemical Society.

Addition of excess CH_3I to a solution of $[Ni^I(tmc)]^+$ results in the rapid loss of the absorption ($\lambda = 360$ nm, $\varepsilon = 4 \times 10^3\ M^{-1}\ cm^{-1}$) and appearance of a less intense band at $\lambda = 346$ nm. A subsequent slower reaction gives rise to the weaker absorbance profile of $[Ni^{II}(tmc)]^{2+}$. The data are interpreted in terms of the formation of an organonickel(II) species followed by a slower hydrolysis with breaking of the Ni–C bond. Kinetic studies under conditions of excess alkyl halide show a dependence according to the equation $-d[Ni^I(tmc)^+]/dt = 2k[Ni(I)][RX]$. The data have been interpreted in terms of a rate-determining one-electron transfer from the nickel(I) species to RX, either by outer-sphere electron transfer or by halogen atom transfer, to yield the alkyl radical R. This reactive intermediate reacts rapidly with a second nickel(I) species:

$$[Ni^I(tmc)]^+ + CH_3I \xrightarrow{k} [Ni^{II}(tmc)]^{2+} + I^- + \cdot CH_3 \qquad (21)$$

$$[Ni^I(tmc)]^+ + CH_3^{\cdot} \xrightarrow{\text{rapid}} [CH_3Ni(tmc)]^+ \qquad (22)$$

The slower hydrolytic decomposition of the $[CH_3Ni(tmc)]^+$ yields CH_4 and $[Ni^{II}(tmc)]^{2+}$. Confirmation of the radical capture by nickel(I) may be illustrated using 6-bromo-1-hexene. One-electron reduction of this species yields the 1-hexanyl radical which rapidly undergoes cyclization to the cyclopentamethyl radical. Further reduction results in 1-hexane and methylcyclopentane. Reaction of $[Ni^I(tmc)]^+$ with $Br(CH_2)_4CHCH_2$ results after hydrolysis in both reduced species as forms with $c\text{-}C_5H_9Me$ predominating. The reaction rate of the nickel(I) species with $CH_2(CH_2)_4CH{=}CH_2$ was evaluated as $6 \times 10^7\ M^{-1}\ sec^{-1}$. In the case of *t*-butyl hydroperoxide, the presence of two, one-electron transfer steps is confirmed by the detection of $[CH_3Ni(tmc)]^+$ [from the decomposition $(CH_3)_3CO \rightarrow (CH_3)_2CO + CH_3$]. The reactivity order observed is methyl < primary < secondary.

The organonickel(II) species formed as intermediates in the reactions above react further (*196*) with alkyl halides with the formation of coupled products, alkanes and alkenes.

$$[RNi(tmc)]^+ + RX \longrightarrow [Ni^{II}(tmc)]^{2+} + (R_2 + RH + R^-H) + X^- \qquad (23)$$

Kinetic dependences are first order with respect to each reactant and reactivity increases in the order shown above with Cl < Br < I. In the case of ethyl iodide, the disproportionation/combination ratio (k_d/k_c) of 0.35 ± 0.04 is identical to that observed by other methods. In the case of the acyclic valeronitrile (*198*) complex,

$$C_2H_4 + C_2H_6 \xleftarrow{k_d} 2CH_2H_5^{\cdot} \xrightarrow{k_c} C_4H_{10} \qquad (24)$$

$[NC(CH_2)_3CH_2Ni(tmc)]^+$, a facile non radical cyclization to cyclopentanone occurs as the hydrolysis reaction proceeds.

$$[NC(CH_2)_3CH_2Ni(tmc)]^+ + 2H_2O \xrightarrow{k_c}$$
$$[Ni^{II}(tmc)]^{2+} + c\text{-}(CH_2)_4C{=}O + NH_3 + HO^- \qquad (25)$$

In this system a very stable dimeric species is formed via reaction of a second nickel(I) species complexing to the cyano group. Of interest is the fact that the cyclization rate k_c is $\sim$4 orders of magnitude slower than that for the free radical alone.

Electron transfer reactions of the organonickel species with $[Co(dmgH)_2]$ have been described (*197*). Reaction rates are very high ($k > 2 \times 10^6\ M^{-1}\ sec^{-1}$) and cannot be measured by the stopped-flow technique. However, the blue organocobalt(I) products have been characterized by ^1H NMR methods. Rapid reactions have also been observed (*193*) in the oxidations of $[Ni^IMe_6[14]4,11\text{-dieneN}_4]^+$ and $[Ni^IMe_6[14]aneN_4]^+$ by $[M(bipy)_3]^{3+}$ (M = Co, Cr, or Fe), $[Ru(NH_3)_6]^{3+}$, and $[Co(en)_3]^{3+}$.

VI. List of Abbreviations

[9]aneN$_3$, 1,4,7-Triazacyclononane
[10]aneN$_3$, 1,4,7-Triazacyclodecane
[11]aneN$_3$, 1,4,8-Triazacycloundecane
[12]aneN$_4$, 1,4,7,10-Tetraazadodecane
[13]aneN$_4$, 1,4,7,10-Tetraazatridecane
[14]aneN$_4$, 1,4,8,11-Tetraazatetradecane
iso[14]aneN$_4$, 1,4,7,11-Tetraazatetradecane
[15]aneN$_4$, 1,4,8,12-Tetraazapentadecane
[16]aneN$_4$, 1,5,9,13-Tetraazahexadecane
[15]aneN$_5$, 1,4,7,10,13-Pentaazapentadecane
[16]aneN$_5$, 1,4,7,10,14-Pentaazahexadecane
[17]aneN$_5$, 1,4,7,11,14-Pentaazaheptadecane
[18]aneN$_6$, 1,4,7,10,13,16-Hexaazaoctadecane
Me$_2$[14]aneN$_4$, 5,12-Dimethyl-1,4,8,11-tetraazatetradecane
Et$_2$[14]aneN$_4$, 5,12-Diethyl-1,4,8,11-tetraazatetradecane
N-Me$_4$[14]aneN$_4$tmc, 1,4,8,11-Tetramethyl-1,4,8,11-tetraazacyclotetradecane
Me$_6$[14]aneN$_4$, 5,7,7,12,14,14-Hexamethyl-1,4,8,11-tetraazacyclotetradecane
N-Me$_4$Me$_6$[14]aneN$_4$, 1,4,5,7,7,8,11,12,14,14-Decamethyl-1,4,8,11-tetraazacyclotetradecane
Me$_2$[14]dieneN$_4$, 1,2-Dimethyl-1,4,8,11-tetraazacyclotetradeca-1,2-diene

Me_4[14]1,3,8,10-tetraeneN_4, 1,4,8,11-Tetraazacyclotetradeca-1,3,8,10-tetraene
Me_6[14]4,11-dieneN_4, 5,7,7,12,14,14-Hexamethyl-1,4,8,11-tetraazacyclotetradeca-4,11-diene
[14]ane$N_4CH_2CH_2$py, 6-Ethyl-2′-pyridine-1,4,8,11-tetraazacyclotetradecane
[13]ane$N_4C_6H_5OH$, 5:2′-Phenol-1,4,7,10-tetraazacyclotridecane
[14]ane$N_4C_6H_5OH$, 5:2′-Phenol-1,4,8,11-tetraazacyclotetradecane
Aib_3, Tri-α-aminoisobutyric acid

bpo, *syn*-2-Benzoylpyridine oxime
bpy, 2,2′-Bipyridyl
$bpyO_2$, 2,2′-Bipyridine-1,1′dioxide

$dapdH_2$, 2,6-Diacetylpyridine dioxime
$dmgH_2$, Dimethylglyoxime
(DOH)pn, 3,9-Dimethyl-4,8-diazaundeca-3,8-diene-2,10-dione dioxime
$dpgH_2$, Diphenylglyoxime

$edtaH_4$, 1,2-Diaminoethane-*N*,*N*,*N*′,*N*′-tetraacetic acid
en, 1,2-Diaminoethane

G_3a, Triglycineamide
G_3, Triglycine
G_4, Tetraglycine
G_5, Pentaglycine

Me_2LH_2, 3,14-Dimethyl-4,7,10,13-tetraazahexadeca-3,13-diene-2,15-dione dioxime
$Me_2L'H$, 3-Methyl-4,7,10,13,16-pentaazahexadeca-3-ene-2-one oxime

phen, 1,10-Phenanthroline
py, Pyridine

TACNTA, 1,4,7-Triazacyclononane-*N*,*N*′,*N*″-triacetate
terpy, 2,2′:6′2″-Terpyridyl
2,2,2-tet, 1,4,7,10-Tetraazadecane
1,3,2-tet, 1,4,8,11-Tetraazaundecane
[12]dioxoane, 1,4,7,10-Tetraazadodecane-2,6-dione
[13]dioxoane, 1,4,7,10-Tetraazatridecane-11,13-dione
[14]dioxoaneN_4, 1,4,8,11-Tetraazatetradecane-5,7-dione
[15]dioxoaneN_4, 1,4,8,12-Tetraazapentadecane-9,11-dione
[16]oxoaneN_5, 1,4,7,10,13-Pentaazahexadecane-14-one
[16]dioxoaneN_5, 1,4,7,10,13-Pentaazahexadeca-14,16-dione
[13]dioxoane$N_4CH_2CH_2$py, 12-Ethyl-1′-pyridine-1,4,7,10-tetraazatridecane-11,13-dione
[13]dioxoane$N_4CH_2CH_2$pyO, 12-Ethyl-2′-pyridine-*N*-oxide-1,4,7,10-tetraazatridecane-11,13-dione
[14]dioxoane$N_4CH_2CH_2$py, 6-Ethyl-2′-pyridine-1,4,8,11-tetraazatetradecane-5,7-dione
[16]dioxoane$N_5CH_2XH_2$py, 15-Ethyl-2′-pyridine-1,4,7,10,13-pentaazahexadeca-4,16-dione

ACKNOWLEDGMENTS

The authors would like to acknowledge Professor J. H. Espenson for the provision of material prior to publication. This work was supported in part by the National Science Foundation (Grant No. 84-06113), which is gratefully acknowledged.

REFERENCES

1. Lancaster, J. R., *Science* **216,** 1324 (1982).
2. Albracht, S. P. J., Graf, E. C., and Thauer, R. K. *FEBS Lett* **140,** 311 (1982).
3. LeGall, J., Ljundahl, P. O., Moura, I., Peck, H. D., Xavier, A. V., Moura, J. J., Teixera, M., Huynh, B. H., and Der Vartanian, D. V., *Biochem. Biophys. Res. Commun.* **106,** 610 (1982).
4. Moura, J. J. G., Moura, I., Huynh, B. H., Krueger, H. J., Teixeira, M., DuVarney, R. C., Der Vartanian, D. V., Xavier, A. V., Peck, H. D., and Le Gall, J., *Biochem, Biophys. Res. Commun.* **108,** 1388 (1982).
5. Cammack, R., Patil, D., Aguirre, R., and Hatchikian, E. V., *FEBS Lett.* **142,** 289 (1982).
6. Albracht, S. P. J., Kalkman, M. L., and Slater, E. C., *Biochim. Biophys. Acta* **724,** 309 (1983).
7. Albracht, S. P. J., Van der Zwaan, J. W., and Fontijn, R. D., *Biochim. Biophys. Acta* **766,** 245 (1984).
8. Van der Zwaan, J. W., Albracht, S. P. J., Fontijn, R. D., and Slater, E. C., *FEBS Lett.* **179,** 271 (1985).
9. Nag, K., and Chakravorty, A., *Coord. Chem. Rev.* **33,** 87 (1980).
10. Haines, R. I., and McAuley, A., *Coord. Chem. Rev.* **39,** 77 (1981).
11. Margerum, D. W., Cayley, G. R., Weatherburn, D. C., and Pagenkopf, G. K., *Coord. Chem.* **2,** 1 (1978).
12. Wilkins, R. G., *Comments Inorg. Chem.* **2,** 187 (1983).
13. Merbach, A. E., *Pure Appl. Chem.* **54,** 1479 (1982).
14. Dwyer, F. P., and Gyarfas, E. C. J., *Proc. R. Soc. New South Wales* **83,** 232 (1949).
15. Wilkins, R. G., and Williams, M. J. G., *J. Chem. Soc.* 1763 (1967).
16. Maki, A. H., Edelstein, N., Davison, A., and Holm, R. H., *J. Am. Chem. Soc.* **86,** 4580 (1964).
17. Maki, A. H., and McGarvey, B. R., *J. Chem. Phys.* **29,** 31 (1958).
18. Drago, R. S., and Baucom, E. I., *Inorg. Chem.* **11,** 2064 (1972).
19. Peacock, R. D., and Stewart, B., *Coord. Chem. Rev.* **46,** 129 (1982).
20. Lati, J., and Meyerstein, D., *Inorg. Chem.* **11,** 2393 (1972).
21. Lati, J., and Meyerstein, D., *Inorg. Chem.* **11,** 2397 (1972).
22. Fried, I., and Meyerstein, D., *Isr. J. Chem.* **8,** 865 (1970).
23. Liu, H., Shen, W., Quayle, W. H., and Lunsford, J. H., *Inorg. Chem.* **23,** 4553 (1984).
24. Shen, W., and Lunsford, J. H., *Inorg. Chim. Acta* **102,** 199 (1985).
25. Yamashita, M., Nonaka, Y., Kida, S., Hamane, Y., and Aoki, R., *Inorg. Chim. Acta* **52,** 43 (1981).
26. Cooper, D. A., Higgins, S. J., and Levason, W., *J. Chem. Soc. Dalton Trans.* 2131 (1983).
27. Papavassiliou, G. C., and Layek, D., *Z. Naturforsch* **37B,** 1406 (1982).
28. Yamashita, M., and Murase, I., *Inorg. Chim. Acta* **97,** L43 (1985).
29. Wells, C. F., and Fox, D., *J. Chem. Soc. Dalton Trans.* 1492 (1977).

30. Prasad, R., and Scaife, D. B., *J. Electroanal. Chem.* **84,** 373 (1977).
31. Brodovitch, J. C., Haines, R. I., and McAuley, A., *Can. J. Chem.* **59,** 1610 (1981).
32. Szalada, D. J., Macartney, D. H., and Sutin, N., *Inorg. Chem.* **23,** 3473 (1984).
33. Wieghardt, K., Walz, W., Nuber, B., Weiss, J., Ozarowski, A., Stratemeier, H., and Reinen, D., *Inorg. Chem.* **25,** 1650 (1986).
34. Wada, A., Sakabe, N., and Tanaka, J., *Acta Crystallogr. Sect. B* **B32,** 1121 (1976).
35. Simek, M., *Collect. Czech. Chem. Commun.* **27,** 220 (1962).
36. Panda, R. K., Acharya, S., Neogi, G., and Ramaswamy, D., *J. Chem. Soc. Dalton Trans.* 1225 (1983).
37. Neogi, G., Acharya, S., Panda, R. K., and Ramaswamy, D., *J. Chem. Soc. Dalton Trans.* 1233 (1983).
38. Davis, D. G., and Boudreaux, E. A., *J. Electroanal. Chem.* **8,** 434 (1964).
39. Marov, I. N., Ivanova, E. K., Panfilov, A. T., and Luneva, N. P., *Z. Neorg. Khim.* **20,** 123 (1975); *J. Inorg. Chem.* **20,** 67 (1975).
40. Acharya, S., Neogi, G., Panda, R. K., and Ramaswamy, D. *J. Chem. Soc. Dalton Trans.* 1471 (1984).
41. Baral, S., and Lappin, A. G., *J. Chem. Soc. Dalton Trans.* 2213 (1985).
42. Lati, J., and Meyerstein, D., *Isr. J. Chem.* **10,** 735 (1972).
43. Baucom, E. I., and Drago, R. S., *J. Am. Chem. Soc.* **93,** 6469 (1971).
44. Sproul, G., and Stucky, G. D., *Inorg. Chem.* **12,** 2898 (1973).
45. Mohanty, J. G., Singh, R. P., and Chakravorty, A., *Inorg. Chem.* **14,** 2178 (1975).
46. Mohanty, J. G., and Chakravorty, A., *Inorg. Chem.* **15,** 2912 (1976).
47. Singh, A. N., Singh, R. P., Mohanty, J. G., and Chakravorty, A., *Inorg. Chem.* **16,** 2597 (1977).
48. Singh, A. N., *Indian J. Chem.* (1987).
49. Singh, A. N., *Synth. React. Inorg. Met. Org. Chem.* **16,** 279 (1986).
50. Singh, A. N., *Synth. React. Inorg. Met. Org. Chem.* **16,** 433 (1986).
51. Korvenranta, J., Saarinen, H., and Näsäkkälä, M., *Inorg. Chem.* **21,** 4297 (1982).
52. Saarinen, H., Korvenranta, J., and Näsäkkälä, E., *Acta Chem. Scand.* **A34,** 443 (1980).
53. Korvenranta, J., Saarinen, H., and Näsäkkälä, E., *Finn. Chem. Lett.* 81 (1979).
54. Heaney, P. J., Lappin, A. G., Peacock, R. D., and Stewart, B., *J. Chem. Soc. Chem. Commun.* 769 (1980).
55. Lappin, A. G., Laranjeira, M. C. M., and Peacock, R. D., *Inorg. Chem.* **22,** 786 (1983).
56. Lappin, A. G., and Laranjeira, M. C. M., *J. Chem. Soc. Dalton Trans.* 1861 (1982).
57. Chakravorty, A., *Isr. J. Chem.* **25,** 99 (1985).
58. Chakravorty, A., *Comments Inorg. Chem.* **4,** 1 (1985).
59. McAuley, A., and Preston, K. F., *Inorg. Chem.* **22,** 2111 (1983).
60. Singh, A. N., and Chakravorty, A., *Inorg. Chem.* **19,** 969 (1980).
61. Bentgen, J. M., Gimpert, H.-R., and Zelewsky, A., *Inorg. Chem.* **22,** 3576 (1983).
62. Olsen, D. C., and Vasilevikis, J., *Inorg. Chem.* **8,** 1611 (1969).
63. Gore, E. S., and Busch, D. H., *Inorg. Chem.* **12,** 1 (1973).
64. Lovecchio, F. V., Gore, E. S., and Busch, D. H., *J. Am. Chem. Soc.* **96,** 3109 (1974).
65. Busch, D. H., *Acc. Chem. Res.* **11,** 392 (1978).
66. Busch, D. H., Pillsbury, D. G., Lovecchio, F. V., Tait, A. M., Hung, Y., Jackels, S., Rakowski, M. C., Schammel, W. P., and Martin, L. Y., *Electrochem. Stud. Biol. Syst.* **38,** 32 (1977).
67. Hinz, F. P., and Margerum, D. W., *Inorg. Chem.* **13,** 2941 (1974).
68. Anachini, A., Fabbrizzi, L., Paoletti, P., and Clay, R. M., *Inorg. Chim. Acta* **24,** L21 (1977).
69. Fabbrizzi, L., *J. Chem. Soc. Dalton Trans.* 1857 (1979).

70. Sabatini, L., and Fabbrizzo, L., *Inorg. Chem.* **18,** 438 (1979).
71. Wilkins, R. G., Yelin, R. E., Margerum, D. W., and Weatherburn, D. C., *J. Am. Chem. Soc.* **91,** 4326 (1969).
72. Fabbrizzi, L., *J. Chem. Soc. Chem. Commun.* 1063 (1979).
73. Bencini, A., Fabbrizzi, L., and Poggi, A., *Inorg. Chem.* **20,** 2544 (1981).
74. Desideri, A., Raynor, B., and Poon, C.-K., *J. Chem. Soc. Dalton Trans.* 2051 (1977).
75. Haines, R. I., and McAuley, A., *Inorg. Chem.* **19,** 719 (1980).
76. McAuley, A., Morton, J. R., and Preston, K. F., *J. Am. Chem. Soc.* **104,** 7561 (1982).
77. Cohen, H., Kirchenbaum, L. J., Zeigerson, E., Jaacobi, M., Fuchs, E., Gingburg, G., and Meyerstein, D. *Inorg. Chem.* **18,** 2763 (1979).
78. Zeigerson, E., Ginzburg, G., Shwartz, N., Luz, Z., and Meyerstein, D., *J. Chem. Soc. Chem. Commun.* 241 (1979).
79. Zeigerson, E., Ginzburg, G., Becker, J. Y., Kirschenbaum, L. J., Cohen, H., and Meyerstein, D., *Inorg. Chem.* **20,** 3918 (1981).
80. Zeigerson, E., Bar, I., Berstein, J., Kirschenbaum, L. J., and Meyerstein, D., *Inorg. Chem.* **21,** 73 (1982).
81. Ho, T., Sugimoto, M., Toriumi, K., and Ito, H., *Chem. Lett.* 1477 (1981).
82. Yamaduta, M., Toriumi, K., and Ito, T., *Acta Crystallogr. Sect. C* **C41,** 1607 (1985).
83. Bosnich, B., Mason, R., Pauling, P. J., Robertson, G. B., and Robe, M. L., *J. Chem. Soc. Chem. Commun.* 97 (1965).
84. Barefield, E. K., and Mocella, M. T., *J. Am. Chem. Soc.* **97,** 4238 (1975).
85. Maruthamuthu, P., Patterson, L. K., and Ferraudi, G., *Inorg. Chem.* **17,** 3157 (1978).
86. Jaacobi, M., Meyerstein, D., and Lilie, J., *Inorg. Chem.* **18,** 429 (1979).
87. Morliere, P., and Patterson, L. K., *Inorg. Chem.* **20,** 1458 (1981).
88. Morliere, P., and Patterson, L. K., *Inorg. Chem.* **21,** 1837 (1982).
89. Ulman, A., Cohen, H., and Meyerstein, D., *Inorg. Chim. Acta* **64,** L127 (1982).
90. Cohen, H., Nutkovich, M., Meyerstein, D., and Shusterman, A., *Inorg. Chem.* **23,** 2361 (1984).
91. McElroy, F. C., and Dabrowiak, J. C., *J. Am. Chem. Soc.* **98,** 7112 (1976).
92. Fabbrizzi, L., and Poggi, A., *J. Chem. Soc. Chem. Commun.* 646 (1980).
93. Kodama, M., and Kimura, E., *J. Chem. Soc. Dalton Trans.* 694 (1981).
94. Hay, R. W., Bembi, R., and Sommerville, W., *Inorg. Chim. Acta* **59,** 157 (1982).
95. Fabbrizzi, L., Perotti, A., and Poggi, A., *Inorg. Chem.* **22,** 1411 (1983).
96. Kimura, E., Koike, T., Machida, R., Nagai, R., and Kodama, M., *Inorg. Chem.* **23,** 4181 (1984).
97. Fabbrizzi, L., Kaden, T. A., Perotti, A., Seghi, B., and Liselotti, S., *Inorg. Chem.* **25,** 321 (1986).
98. Fabbrizzi, L., Licchelli, M., Perotti, A., Poggi, A., and Soresi, S., *Isr. J. Chem.* **25,** 112 (1985).
99. Kimura, E., *Pure Appl. Chem.* **58,** 1461 (1986).
100. Hitaka, Y., Koike, T., and Kimura, E., *Inorg. Chem.* **25,** 402 (1986).
101. Rakowski, M. C., Rycheck, M., and Busch, D. H., *Inorg. Chem.* **14,** 1194 (1975).
102. Kimura, E., Machida, R., and Kodama, M., *J. Am. Chem. Soc.* **106,** 5497 (1984).
103. Kushi, Y., Machida, R., and Kimura, E., *J. Chem. Soc. Chem. Commun.* 216 (1985).
104. Machida, R., Kimura, E., and Kushi, Y., *Inorg. Chem.* **25,** 3461 (1986).
105. Kimura, E., and Machida, R., *J. Chem. Soc. Chem. Commun.* 499 (1984).
106. Wieghardt, K., Schmidt, W., Herrmann, W., Küppers, H. J., *Inorg. Chem.* **22,** 2953 (1983).
107. McAuley, A., Norman, P. R., and Olubuyide, O., *Inorg. Chem.* **23,** 1939 (1984).
108. Buttafava, A., Fabbrizzi, L., Perotti, A., Poggi, A., Poli, G., and Seglu, B., *Inorg. Chem.* **25,** 1456 (1986).

109. Zompa, L. J., and Margulis, T. N., *Inorg. Chim. Acta* **28,** L157 (1978).
110. Margerum, D. W., and Dukes, G. R., *In* "Metal Ions in Biological Systems" (H. Siegel, ed.), Vol. 1, p. 157. Dekker, New York, 1974.
111. Freeman, H. C., Guss, J. M., and Sinclair, R. L., *J. Chem. Soc. Chem. Commun.* 485 (1968).
112. Paniago, E. B., Weatherburn, D. C., and Margerum, D. W., *J. Chem. Soc. Chem. Commun.* 1427 (1971).
113. Bossu, F. P., and Margerum, D. W., *J. Am. Chem. Soc.* **98,** 4003 (1976).
114. Bossu, F. P., Paniago, E. B., Margerum, D. W., Kirksey, S. T., and Kurtz, J. L., *Inorg. Chem.* **17,** 1034 (1978).
115. Sakurai, T., and Nakahara, A., *Inorg. Chim. Acta* **34,** L243 (1979).
116. Bossu, F. P., and Margerum, D. W., *Inorg. Chem.* **16,** 1210 (1977).
117. Youngblood, M. P., and Margerum, D. W., *Inorg. Chem.* **19,** 3068 (1980).
118. Lappin, A. G., Murray, C. K., and Margerum, D. W., *Inorg. Chem.* **17,** 1630 (1978).
119. Sugiura, Y., and Mino, Y., *Inorg. Chem.* **18,** 1336 (1979).
120. Sakurai, T., Hongo, J.-I., Nakahara, A., and Nakao, Y., *Inorg. Chim. Acta* **46,** 205 (1980).
121. Sugiura, Y., Kuwahara, J., and Suzuki, T., *Biochem. Biophys. Res. Commun.* **115,** 878 (1983).
122. Murray, C. K., and Margerum, D. W., *Inorg. Chem.* **21,** 3501 (1982).
123. Kervan, G. E., and Margerum, D. W., *Inorg. Chem.* **24,** 3245 (1985).
124. Jacobs, S. A., and Margerum, D. W., *Inorg. Chem.* **23,** 1195 (1984).
125. Subak, E. J., Loyola, V. M., and Margerum, D. W., *Inorg. Chem.* **24,** 4350 (1985).
126. Pappenhagen, T. L., Kennedy, W. R., Bowers, C. P., and Margerum, D. W., *Inorg. Chem.* **24,** 4356 (1985).
127. Lati, J., and Meyerstein, D., *Int. J. Radiat. Phys. Chem.* **7,** 611 (1975).
128. Lati, J., and Meyerstein, D., *J. Chem. Soc. Dalton Trans.* 1105 (1978).
129. Lati, J., Koresh, J., and Meyerstein, D., *Chem. Phys. Lett.* **33,** 286 (1975).
130. Fuchs, E., Ginsburg, G., Lati, J., and Meyerstein, D., *J. Electroanal. Chem.* **73,** 83 (1976).
131. Van der Merwe, M. J., Boeyens, J. C. A., and Hancock, R. D., *Inorg. Chem.* **22,** 3489 (1983).
132. Hall, R. D., *J. Am. Chem. Soc.* **29,** 692 (1907).
133. Baker, L. C. W., and Weakley, T. J. R., *J. Inorg. Nucl. Chem.* **28,** 447 (1966).
134. Roy, A., and Chaudhury, M., *Bull. Chem. Soc. Jpn.* **56,** 2827 (1983).
135. Bhattacharya, S., Mukherjee, R., and Chakravorty, A., *Inorg. Chem.* **25,** 3448 (1986).
136. Pappenhagen, T. L., and Margerum, D. W., *J. Am. Chem. Soc.* **107,** 4576 (1985).
137. Barefield, E. K., and Busch, D. H., *J. Chem. Soc. Chem. Commun.* 523 (1970).
138. Whitburn, K. D., and Laurence, G. S., *J. Chem. Soc. Dalton Trans.* 139 (1979).
139. Fairbank, M. G., and McAuley, A., *Inorg. Chem.* **25,** 1233 (1986).
140. Fairbank, M. G., and McAuley, A., *Inorg. Chem.* **26,** 2844 (1987).
141. Margerum, D. W., *ACS Symp. Ser.* (198), 8 (1982).
142. Brodovitch, J. C., and McAuley, A., *Inorg. Chem.* **20,** 1667 (1981).
143. Endicott, J. F., Durham, B., and Kumar. K., *Inorg. Chem.* **21,** 2437 (1982).
144. Fairbank, M. G., and McAuley, A., to be published.
145. Macartney, D. H., and McAuley, A., *Can. J. Chem.* **60,** 2625 (1982).
146. Fairbank, M. G., McAuley, A., Norman, P. R., and Olubuyide, O., *Can. J., Chem.* **63,** 2983 (1985).
147. Macartney, D. H., and McAuley, A., *Can. J. Chem.* **61,** 103 (1983).
148. McAuley, A., Macartney, D. H., and Oswald, T., *J. Chem. Soc. Chem. Commun.* 274 (1982).

149. McAuley, A., Norman, P. R., and Olubuyide, O., *J. Chem. Soc. Dalton Trans.* 1501 (1984).
150. Marcus, R. A., *Annu. Rev. Phys. Chem.* **15,** 155 (1964).
151. Sutin, N., *Acc. Chem. Res.* **15,** 275 (1982).
152. Sutin, N., *Prog. Inorg. Chem.* **30,** 441 (1983).
153. Fairbank, M. G., Norman, P. R., and McAuley, A., *Inorg. Chem.* **24,** 2639 (1985).
154. Cooksey, C. J., and Tobe, M. L., *Inorg. Chem.* **17,** 1558 (1978).
155. Hay, R. W., Norman, P. R., House, D. A., and Poon, C. K., *Inorg. Chim. Acta* **48,** 81 (1981).
156. McAuley, A., Olubuyide, O., Spencer, L., and West, P. R., *Inorg. Chem.* **23,** 2594 (1984).
157. Braunschweig, B., and Sutin, N., *Inorg. Chem.* **18,** 1731 (1979).
158. Macartney, D. H., McAuley, A., and Olubuyide, O. A., *Inorg. Chem.* **24,** 307 (1985).
159. Macartney, D. H., and Sutin, N., *Inorg. Chem.* **22,** 3530 (1983).
160. Singh, A. N., Mohanty, J. G., and Chakravorty, A., *Inorg. Nucl. Chem. Lett.* **14,** 441 (1978).
161. Allan, A. E., Lappin, A. G., and Laranjeira, M. C. M., *Inorg. Chem.* **23,** 477 (1984).
162. Munn, S. F., Lannon, A. M., Laranjeira, M. C. M., and Lappin, A. G., *J. Chem. Soc. Dalton Trans.* 1371 (1984).
163. Lappin, A. G., Martone, D. P., and Osvath, P., *Inorg. Chem.* **24,** 4187 (1985).
164. Owens, G. D., Phillips, D. A., Czarnecki, J. J., Raycheba, J. M. T., and Margerum, D. W., *Inorg. Chem.* **23,** 1345 (1984).
165. Murray, C. K., and Margerum, D. W., *Inorg. Chem.* **22,** 463 (1983).
166. Margerum, D. W., *Pure Appl. Chem.* **55,** 23 (1983).
167. Acharya, S., Neogi, G., and Panda, R. K., *Inorg. Chem.* **23,** 4393 (1984).
168. Neogi, G., Acharya, S., Panda, R. K., and Ramaswamy, D., *J. Chem. Soc. Dalton Trans.* 1239 (1983).
169. Neogi, G., Acharya, S., Panda, R. K., and Ramaswamy, D., *Int. J. Chem. Kinet.* **15,** 521 (1983).
170. Acharya, S., Neogi, G., Panda, R. K., and Ramaswamy, D., *Bull. Chem. Soc. Jpn.* **56,** 2814 (1983).
171. Acharya, S., Neogi, G., Panda, R. K., and Ramaswamy, D., *Bull. Chem. Soc. Jpn.* **56,** 2921 (1983).
172. Sahu, R., Neogi, G., Acharya, S., and Panda, R. K., *Int. J. Chem. Kinet.* **15,** 823 (1983).
173. Macartney, D. H., and McAuley, A., *Inorg. Chem.* **22,** 2062 (1983).
174. Macartney, D. H., and McAuley, A., *J. Chem. Soc. Dalton Trans.* 103 (1984).
175. Lappin, A. G., Laranjeira, M. C. M., and Youde-Owei, L., *J. Chem. Soc. Dalton Trans.* 721 (1981).
176. Awanya, F. A., Thesis, University of Notre Dame, 1984.
177. Jönsson, L., *Acta Chem. Scand.* **B37,** 761 (1983).
178. Amano, C., and Fujiwara, S., *Bull. Chem. Soc. Jpn.* **46,** 1379 (1973).
179. Tanaka, N., Ogata, T., and Niizuma, S., *Inorg. Nucl. Chem. Lett.* **8,** 965 (1972).
180. Tanaka, N., and Sato, Y., *Inorg. Nucl. Chem. Lett.* **4,** 487 (1968).
181. Dietrich-Buchecker, C. D., Kern, J. M., and Sauvage, J. P., *J. Chem. Soc. Chem. Commun.* 760 (1985).
182. Jubran, N., Ginzburg, G., Cohen, H., and Meyerstein, D., *J. Chem. Soc. Chem. Commun.* 517 (1982).
183. Jubran, N., Ginzburg, G., Cohen, H., Koresch, Y., and Meyerstein, D., *Inorg. Chem.* **24,** 251 (1985).
184. Gagné, R. R., and Ingle, D. M., *Inorg. Chem.* **20,** 420 (1981).
185. Jubran, N., Cohen, H., and Meyerstein, D., *Isr. J. Chem.* **25,** 118 (1985).

186. Gagné, R. R., and Ingle, D. M., *J. Am. Chem. Soc.* **102,** 1444 (1980).
187. Becker, J. U., Kerry, J. B., Pletcher, D., and Rosas, R., *J. Electroanal. Chem. Interfacial Electrochem.* **117,** 87 (1981).
188. Gosden, C., Kerr, J. B., Pletcher, D., and Rosas, R., *J. Electroanal. Chem. Interfacial Electrochem.* **117,** 101 (1981).
189. Bakac, A., and Espenson, J. H., *J. Am. Chem. Soc.* **108,** 713 (1986).
190. Lewis, J., and Schroeder, M., *J. Chem. Soc. Dalton Trans.* 1085 (1982).
191. Ansell, C. W. G., Lewis, J., Raithby, P. R., Ramsden, J. N., and Schroeder, M. J., *Chem. Soc. Chem. Commun.* 546 (1982).
192. Constable, E. C., Lewis, J., Liptrot, M. C., Raithby, P. R., and Schroeder, M., *Polyhedron* **2,** 301 (1983).
193. Tait, A. M., Hoffman, M. Z., and Hayon, E., *Inorg. Chem.* **15,** 934 (1976).
194. Endicott, J. F., and Durham, B., *In* "Coordination Chemistry of Macrocyclic Compounds" (G. A. Melsor, ed.), p. 393. Plenum, New York, 1979.
195. Fabbrizzi, L., Micheloni, M., and Paoletti, P., *Inorg. Chem.* **19,** 535 (1980).
196. Bakac, A., and Espenson, J. H., *J. Am. Chem. Soc.* **108,** 719 (1986).
197. Ram, M. S., Bakac, A., and Espenson, J. H., *Inorg. Chem.* **25,** 3267 (1986).
198. Bakac, A., and Espenson, J. H., *J. Am. Chem. Soc.* **108,** 5353 (1986).